Available online at www.ijournalse.org

Emerging Science Journal

(ISSN: 2610-9182)

Vol. 8, No. 6, December, 2024

Leveraging Feature Sets and Machine Learning for Enhanced Energy Load Prediction: A Comparative Analysis

Fernando Pedro Silva Almeida [1*], Mauro Castelli [1], Nadine Côrte-Real [1]

[1] NOVA Information Management School (NOVA IMS), Universidade NOVA de Lisboa, Campus de Campolide. 1070-312, Lisboa, Portugal.

Abstract

Accurate cooling consumption forecasts are crucial for optimizing energy management, storage, and overall efficiency in interconnected HVAC systems. Weather conditions, building characteristics, and operational parameters significantly impact prediction accuracy. Since meteorological conditions highly influence cooling demand, leveraging external air data and user metrics offers a promising approach to estimate a building's hourly cooling energy usage. This study addresses the gap in existing research by comprehensively analyzing the performance of various machine learning algorithms, including ensemble learning and deep learning models, to improve prediction accuracy. By leveraging weather conditions, building characteristics, and operational parameters, we aim to predict cooling consumption across multiple systems (Cooling Ceiling, Ventilation, Free Cooling, and Total Cooling). Data from four weather stations, encompassing diverse features relevant to the European Central Bank (ECB) building's cooling consumption in Frankfurt, were employed. Our methodology includes the use of K-Nearest Neighbor, Decision Tree, Support Vector Regression, Linear Regression, Random Forest, Gradient Boosting, XGBoost, Adaboost, Long-Short-Term Memory, and Gated Recurrent Unit. Models. The results consistently demonstrate the superiority of the Random Forest model across different weather stations and feature sets. This model achieved a Mean Squared Error of approximately 0.002-0.003, Mean Absolute Error of around 0.031-0.034, and Root Mean Squared Error of about 0.052-0.069. These findings contribute to improved building cooling load management, promoting insights into optimal energy utilization and sustainable building practices.

Keywords:
Cooling Loads;
Machine Learning;
Deep Learning;
Ensemble Learning;
HVAC Systems.

Article History:

Received:	07	August	2024
Revised:	13	November	2024
Accepted:	19	November	2024
Published:	01	December	2024

1- Introduction

Rising energy demands pose a significant threat to environmental sustainability [1, 2]. The building sector is a significant energy consumer, accounting for 30% of final energy consumption and 26% of CO_2 emissions globally [3], [4]. In the European Union (EU), buildings are responsible for 40% of energy use and 36% of GHG emissions, with 75% of the building stock considered energy-inefficient [5]. To address this challenge, the EU has implemented policies like the Energy Performance of Buildings Directive (EPBD) to promote energy efficiency and renewable energy use. This aligns with the REPowerEU plan, which aims to reduce reliance on fossil fuels and strengthen energy security [5].

Globally, initiatives like the Paris Agreement highlight the urgency of combating climate change [6]. The building industry plays a crucial role by adopting sustainable practices, such as energy-efficient lighting, heating, ventilation, and air conditioning (HVAC) systems, and intelligent building technologies [7–9]. While these measures may involve upfront costs and technological challenges, they are essential for reducing energy consumption and achieving sustainability goals.

[*] **CONTACT**: m20200957@novaims.unl.pt

DOI: http://dx.doi.org/10.28991/ESJ-2024-08-06-01

Proper management of cooling systems is critical for building energy efficiency and accurate prediction and control of cooling loads are essential for optimizing energy use [10]. Machine learning (ML) offers a promising approach to improving cooling forecasts by identifying complex relationships between weather conditions, building characteristics, and occupant behavior [11]. By analyzing historical data from building sensors and weather stations, ML models can learn patterns and trends to predict future cooling needs more accurately.

Integrating ML algorithms into building management systems enables real-time monitoring and control of cooling systems. These systems can adjust cooling parameters based on predicted loads, occupancy patterns, and weather forecasts [12]. Additionally, ML models can identify opportunities for energy-saving measures such as predictive maintenance to reduce equipment failures and strategic scheduling to avoid peak energy use periods [13]. These intelligent systems improve energy control, reduce energy consumption, and enhance occupant comfort.

The application of ML and deep learning (DL) for cooling prediction extends beyond single buildings to large-scale utility management. By collecting data from multiple buildings within a campus or urban area, ML models can identify system-wide patterns and optimize resource allocation for efficient cooling across entire districts [14]. This approach ensures efficient energy utilization without compromising the sustainability of urban environments.

Recent studies have introduced innovative methods and models to improve accuracy and applicability in institutional and commercial buildings. Shin & Do [15] proposed enthalpy-based cooling degree days that consider both latent and sensible heat, offering an alternative to temperature-based methods. Zhao et al. [16] introduced a Backpropagation Artificial Neural Network (BP-ANN) for predicting district cooling system (DCS) energy consumption using readily available weather data. Similarly, Dong et al. [17] proposed a novel hybrid model called Decoupling Weight Decay Adaptive Moment Estimation (DwdAdam)-ILSTM for predicting cooling loads in commercial buildings, with potential applications in daily energy management.

Several cooling systems exist, each addressing specific needs and environmental conditions. Cooling Ceiling (CC) systems utilize convection to cool indoor spaces using chilled water or refrigerant circulated through panels [18]. Cooling Ventilation (CV) systems employ fresh air circulation to remove heat and regulate indoor temperature, often incorporating fans and ducts for optimal air distribution [19]. Free Cooling (FC) systems leverage cool outdoor air to reduce indoor temperatures without mechanical refrigeration, often relying on air or water-side economizers [16]. Finally, Total Cooling (TC) systems combine CC and CV strategies for comprehensive climate control.

This study investigates the application of machine learning, ensemble learning, and deep learning algorithms to predict the energy consumption of various cooling systems—CC, CV, FC, and TC—within the European Central Bank (ECB) office building in Frankfurt. Utilizing data from four weather stations and diverse feature sets identified through correlation analysis, the research advances the current state of knowledge by addressing gaps in existing methods. Unlike previous studies that focused on limited model types or specific features, this study offers a comprehensive analysis of a broad spectrum of algorithms, including Random Forest (RF), Gradient Boosting (GB), XGBoost, Adaboost, Long-Short-Term Memory (LSTM), and Gated Recurrent Unit (GRU). These models are chosen based on their proven effectiveness in handling complex, non-linear relationships and their ability to handle diverse datasets for predicting cooling consumption. Criteria for selection included the models' ability to integrate various feature sets, their performance in previous applications of energy prediction [20-22], and their capacity to leverage ensemble and deep learning techniques for enhanced accuracy. This research offers the following key contributions:

i. ***Integration of Machine Learning Techniques*****:** We present a novel approach that combines machine learning, ensemble learning, and deep learning algorithms for predicting energy consumption in cooling systems. This approach can potentially optimize indoor temperature regulation and improve building energy efficiency.

ii. ***Enhanced Model Robustness and Adaptability*****:** By utilizing data from four distinct weather stations and diverse feature sets, we aim to develop robust and adaptable predictive models that provide accurate and reliable energy consumption forecasts across varying environmental conditions.

iii. ***Improved Sustainability Efforts*****:** By gaining comprehensive insights into CC, CV, FC, and TC systems, this work aims to contribute to sustainability efforts by enabling more efficient resource allocation and energy management strategies within buildings.

The rest of the paper is structured as follows: Section 2 reviews related work, highlighting the strengths and limitations of existing studies. Section 4 outlines the methodology used in this study. Section 5 presents the results and discusses the outcomes of different models. Finally, Section 6 concludes the study.

2- Literature Review

Predicting cooling loads in buildings has been a longstanding research focus due to its crucial role in assessing building energy requirements [15]. Traditional methods, often based on static models and physical principles, struggle to adapt to dynamic changes caused by weather variations, occupant behavior, and temporal factors [17]. Recent research has explored machine learning (ML) and data-driven approaches to address these limitations for developing more accurate and flexible prediction models. Techniques such as Artificial Neural Networks (ANNs), Support Vector Machines (SVMs), and Recurrent Neural Networks (RNNs) have shown promise in identifying non-linear relationships within building energy consumption patterns. Additionally, integrating optimization algorithms with deep learning architectures has demonstrated the potential to improve the accuracy and stability of existing value forecasts.

Several studies highlight the effectiveness of ML and DL techniques for enhancing cooling load and energy consumption prediction in office buildings. For instance, Fan et al. [23] demonstrated that unsupervised deep learning outperforms traditional supervised learning approaches for predicting daily cooling load profiles. Li et al. [24] incorporated attention mechanisms into RNNs for cooling load prediction, achieving improved accuracy and interpretability through declarative principles. Lopes & Lamberts [25] designed a compact ANN model specifically for application in Brazilian office buildings. Amasyali & El-Gohary [26] proposed a machine learning method focused on occupant behavior to assess the performance of different algorithms for energy use prediction.

Beyond office buildings, more sophisticated techniques like hybrid simulations and advanced ML models have been employed to determine cooling energy consumption across diverse building types and regions—for example, Mui et al. [27] proposed a Bayesian regularization integrated simulation model for predicting annual cooling energy demand in subtropical buildings, while Moon et al. [28] designed an ANN model to predict energy use during setback periods in residential buildings. In contrast, Borowski & Zwolińska [29] utilized ANNs and SVMs to forecast cooling energy consumption in a historic hotel building located in southern Poland.

Lu et al. [30] proposes an AutoML-based framework for predicting heating and cooling loads in residential buildings, enhancing prediction accuracy and reducing manual intervention. The framework excels over recent ML models and offers explainable insights into energy load relationships. Also, Liu et al. [31] present a deep learning model using multi-task learning (MTL) for hourly electricity load prediction in commercial buildings. By incorporating temperature prediction as an auxiliary task, the model improves accuracy, reduces overfitting, and benefits from an ensemble technique, showing superior performance and generalization across multiple datasets. Moreover, Zhang et al. [32] introduces an AutoML-based method that develops accurate building energy load prediction models with minimal human input. Evaluating six AutoML frameworks, the method outperforms manual modeling with accuracy improvements of 1.10%–18.66%. AutoGluon and FLAML achieve high accuracy with shorter training times, while AutoKeras underperforms. Similarly, Pavlatos et al. [33] details a Python-coded framework for forecasting electrical load using a recurrent neural network with two simpleRNN layers and a dense layer. Optimized with Adam and tanh loss, the model achieves a root mean square error of 0.033, demonstrating high accuracy and outperforming more complex neural networks. Furthermore, Tsalikidis et al. [34] develops and compares predictive algorithms for one-step-ahead energy load forecasting using historical data from a near Zero Energy Building. The study evaluates various ML algorithms and a hybrid model with ensemble methods, achieving a mean absolute percentage error of 5.39%, surpassing base algorithms and other ensemble approaches. While these studies showcase advancements in modeling techniques, the literature also emphasizes the need for further calibration and efforts to generalize the applicability and accuracy of models across various building types and settings.

Despite advancements in building cooling load identification and prediction, several challenges persist, as summarized in Table 1. These challenges include:

(a) Generalizability: Many existing models are limited in their applicability because they are tailored to specific building types or climates.

(b) Cooling Load Estimation Accuracy: Traditional and some advanced methods often struggle to predict TC loads accurately. This is likely due to their inability to effectively capture the interplay between various cooling strategies (CC, CV, FC).

These limitations highlight the need for developing more comprehensive and generalizable models. Such models should be capable of accurately predicting cooling loads across diverse building types and climates while considering all cooling system types (CC, CV, FC).

Also, to address the theoretical approach of this research, we focus on integrating machine learning (ML) and deep learning (DL) methodologies for predicting building cooling loads. Traditional models based on static principles fall short of capturing the dynamic nature of energy consumption influenced by weather, occupant behavior, and time. Our study employs a theoretical framework that utilizes various ML algorithms, including RF, LSTM, GRU, and ensemble techniques. This approach hypothesizes combining diverse models and contextual data will improve accuracy and adaptability.

Table 1. Summary and Comparison of Existing Techniques

Ref.	Year	Location	Technique	Strength	Limitation
Fan et al. [23]	2017	Office buildings	MLR, DNN, SVR, GBM	Enhances prediction performance by uncovering complex patterns in data	Requires further validation with diverse data sources for broader applicability
Li et al. [24]	2021	Office buildings	Attention RNN	Improves model interpretability and prediction accuracy	Advanced model complexity may hinder widespread adoption by building professionals
Lopes & Lamberts [25]	2018	Office buildings	ANN	A new climate indicator provides a more precise prediction of cooling energy consumption.	Limited to chilled water HVAC systems.
Amasyali & El-Gohary [26]	2021	Office building	CART, EBT, ANN, DNN	Considers occupant behavior, significantly improving prediction accuracy	It needs real-life data validation to capture the complexity of occupant behavior accurately.
Mui et al. [27]	2022	Residential buildings, Healthcare buildings	Hybrid EP-ANN	Effectively predicts energy consumption and identifies energy-saving strategies.	Requires further validation for diverse building types and inclusion of cost analysis
Moon et al. [28]	2015	Residential buildings	ANN	Identifies the most energy-efficient setback temperature with high prediction accuracy.	Requires further validation in actual buildings to ensure stability and address overfitting.
Borowski & Zwolińska [29]	2020	Residential buildings	ANN, SVM	Neural networks demonstrated higher prediction accuracy compared to SVM.	Limited modernization options in historical buildings may hinder the implementation of energy management systems.
Shin & Do [15]	2016	Institutional buildings	CDD	Provides more accurate predictions for cooling energy consumption by considering latent heat	Effectiveness varies based on data periods and building energy use patterns.
Zhao et al. [16]	2023	Office buildings, district comprising multiple buildings	BP-ANN	It offers a simple and convenient method for predicting energy consumption with high accuracy.	Prediction performance is influenced by building thermophysical properties and varying weather parameters.
Dong et al. [17]	2022	Large commercial building	DwdAdam-ILSTM	Improved prediction accuracy and stability compared to the traditional LSTM model	Other ML-based models are not utilized to compare the performance of the proposed model.
Lu et al. [30]	2023	Residential buildings	Liner Regression, XGboost, Naïve Bayes, DNN, GBM	Achieves high prediction accuracy with minimal manual intervention	Requires some level of expert knowledge for implementation
Liu et al. [31]	2023	Commercial buildings	Multi-task learning (MTL) with deep learning	It prevents overfitting and significantly outperforms comparison methods	Requires validation on more diverse datasets
Zhang et al. [32]	2023	Office buildings	RF, DNN, Stacking, Decision Tree	Increases accuracy by 1.10%–18.66% compared to manual modeling.	Some frameworks require longer training times to achieve high accuracy.
Pavlatos et al. [33]	2023	General	RNN	Achieves high accuracy with a root mean square error of 0.033	May not handle extensive datasets or very long-term forecasts as effectively
Tsalikidis et al. [34]	2023	Near Zero Energy building	Hybrid model using ensemble methods	Achieves a mean absolute percentage error of 5.39%, improving upon base algorithms.	Performance evaluation is limited to historical data and specific to one-step-ahead forecasting.

3- Dataset

This study utilizes data from the cooling systems of the ECB building in Frankfurt, Germany. The ECB building is a new, efficiently designed structure equipped with an advanced Building Control System and a network of sensors for comprehensive data collection (see Figure 1).

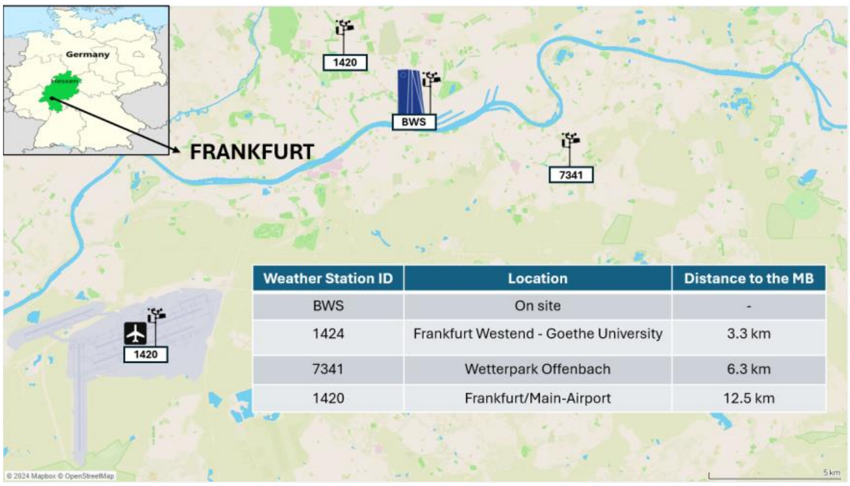

Figure 1. Locations of Weather Stations

The dataset contains various features related to the building's cooling consumption. Additionally, weather data was collected from multiple nearby weather stations and from a station located on top of the building itself. This comprehensive dataset offers valuable insights into the complex interplay between environmental factors and cooling requirements. Currently, this data is primarily used for historical analysis to understand past cooling demands and make general predictions about future needs. However, by leveraging ML techniques, we aim to improve the efficiency and accuracy of these forecasts significantly. ML algorithms can identify complex relationships within the data that might be missed by traditional analysis methods, ultimately leading to more reliable cooling consumption predictions.

3-1- Cooling Consumption Data

The cooling consumption data encompasses various features categorized as meteorological, environmental, and operational factors, which are crucial for predicting energy usage in HVAC systems.

i. ***Meteorological Features:*** These include air temperature, relative humidity, wind speed and direction, precipitation frequency and intensity, and air pressure. They are extracted from weather stations and directly impact cooling energy demand. Higher temperatures and humidity levels generally lead to increased cooling needs. Wind speed and direction significantly affect the effectiveness of CV systems by influencing air movement and cooling rates within buildings. Air pressure variations may also impact HVAC system performance, particularly regarding airflow and distribution.

ii. ***Environmental Features:*** Include observed weather, cloud cover, and visibility. They provide context for interpreting meteorological data and understanding cooling system operations. Observed weather conditions offer insights into prevailing atmospheric conditions that can influence cooling system behavior and energy consumption patterns. Cloud cover data helps determine the level of solar radiation reaching the building on sunny days, thus affecting heat gain. Visibility data can be helpful in inferring potential impacts of air pollution on cooling system efficiency and indoor air quality.

iii. ***Operational Features:*** These features include hour, day, weekday, and month. They provide information on cooling consumption patterns at different times. These features allow for identifying seasonal trends, daily usage patterns, and variations in cooling demand across weekdays. This information is valuable for developing predictive models that support efficient energy management in interconnected HVAC systems.

3-2- Weather Variables from Building Weather Station (BWS)

This study incorporates a comprehensive dataset of meteorological values encompassing temperature, humidity, wind speed, and other parameters for assessing current atmospheric conditions. These factors significantly impact building cooling operations and energy consumption. The data is acquired directly from a weather station positioned atop the ECB skyscraper, providing highly localized and up-to-date weather information specific to the building's immediate environment. The station's elevated location ensures accurate data collection that closely reflects the atmospheric conditions relevant to the building. Building Automation System (BAS) integration further enhances data accessibility and usability. This integration seamlessly transfers and stores weather station data within a centralized system. This configuration allows BAS control rooms to provide building managers and operators with real-time weather data, thus enabling informed decision-making based on current conditions. Additionally, the BAS offers historical data analysis capabilities, allowing users to identify trends and patterns in weather data over time. Accumulating and storing weather data over time facilitates more granular analysis, enabling stakeholders to establish connections between various weather parameters and corresponding cooling system metrics.

3-3- Local Weather Stations

To complement the localized weather data acquired from the station atop the ECB building, this study incorporates data from three additional weather stations: Frankfurt Airport (station 1420), Frankfurt am Main-Westend (station 1424), and Offenbach Weather Park (station 7341). These stations are strategically located at varying distances from the ECB building, enabling the investigation of how broader weather patterns influence cooling and energy demands within the building. The data is obtained from the Deutscher Wetterdienst (DWD), the German National Meteorological Service, and the PIK Potsdam Institute for Climate Impact Research (PIK) – affiliated with the World Data Centre for Climate (WDCC). The DWD and the WDCC are recognized as leading authorities for providing comprehensive and reliable historical weather data. Their extensive network of weather stations allows for capturing a more holistic view of regional weather patterns and trends.

3-4- Data Analysis

Figure 2 illustrates the variations in average hourly outdoor air temperatures across the four weather stations (1420, 1424, 7341, and BWS) throughout 2020, 2021, and 2022, revealing distinct seasonal patterns. This study's weather stations and feature sets provide a comprehensive and representative framework for capturing the variability in cooling demand for the ECB building in Frankfurt. By integrating data from the on-site weather station and three strategically positioned local stations, the study captures various environmental factors, including temperature, humidity, wind speed, and precipitation. This robust approach ensures a thorough representation of both localized and broader meteorological conditions. At the same time, the inclusion of operational features like time-of-day and seasonal patterns further enhances the model's ability to reflect real-world variability in cooling demand. During spring and autumn, temperatures vary slightly across the stations. Station 1424 consistently records the highest average temperatures in both seasons, while 7341 tends to be slightly cooler compared to the other stations. BWS and 1420 show intermediate values, with minimal differences between them. In summer, the temperatures are quite consistent, with station 1424 recording the highest average temperature (around 20.91°C) and BWS the lowest (around 20.10°C). Conversely, winter brings a noticeable drop in temperature across all stations. BWS records the lowest average winter temperature (around 3.89°C), while the other stations—1420, 1424, and 7341—range between 4.26°C and 4.79°C.

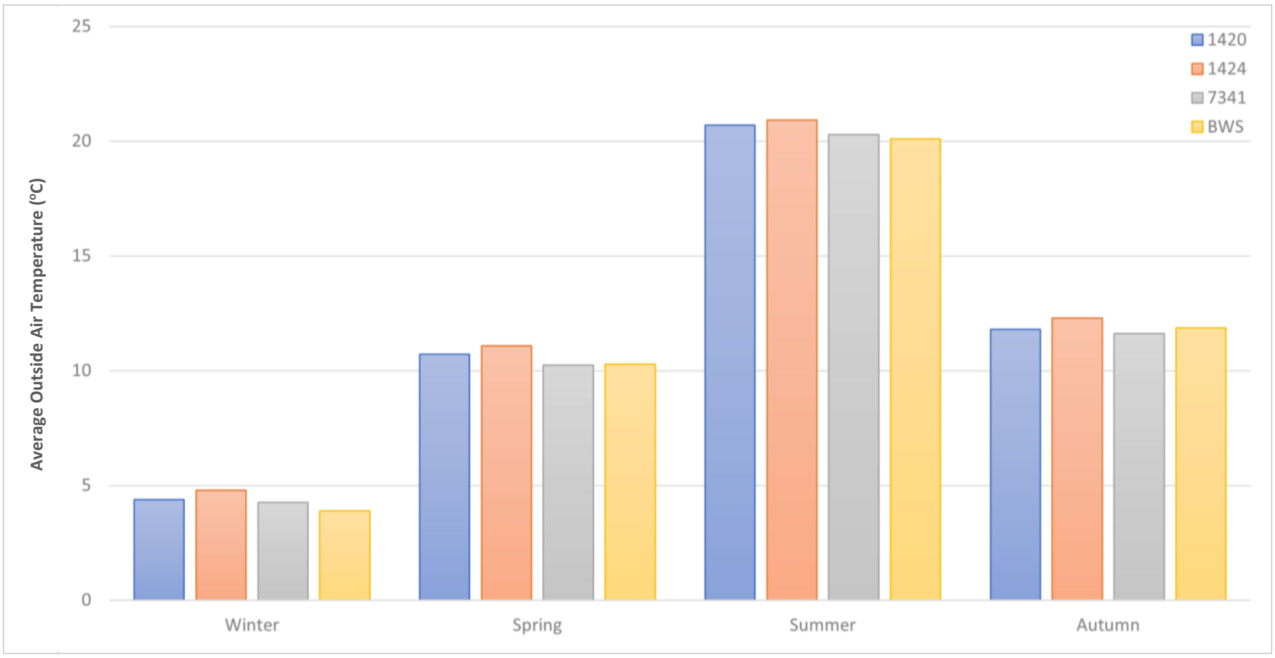

Figure 2. Average air temperature of each weather station across different seasons

Similar to the observed temperature variations, CC exhibits distinct seasonal patterns (Figure 3). Here, CC represents the average cooling demand of the building's system, normalized for factors like building size and occupancy. Summer experiences consistently high average CC, with a significant peak between noon and 7 PM. This coincides with the daily high-temperature period and aligns with a typical occupancy profile in office buildings, where peak occupancy occurs during these afternoon hours. This suggests the cooling system must operate at a higher capacity during this timeframe to maintain comfortable indoor temperatures.

In contrast, spring and autumn exhibit moderate CC values with peaks in the afternoon and early evening. This indicates a lower overall cooling demand compared to summer. Winter has the lowest CC values throughout the day, reflecting minimal cooling needs during this season.

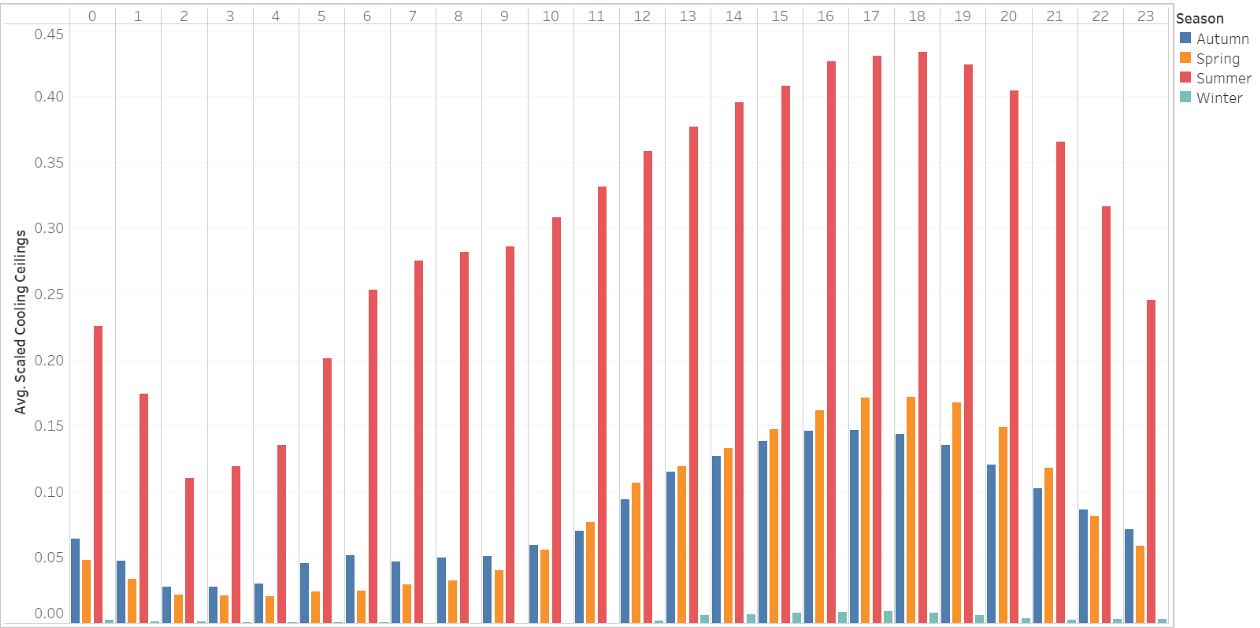

Figure 3. Average of Scaled CC for each Season by Hour

Similar to CC, CV exhibits distinct seasonal patterns (Figure 4). Here, CV represents the average ventilation demand of the building's system, normalized to account for factors influencing ventilation needs. Summer experiences the highest average CV, mainly between noon and 6 PM, reaching a value close to 0.26. This indicates a significant requirement for CV during this period. Autumn and spring exhibit lower ventilation rates, with the highest values (between 0.08 and 0.12) occurring in the afternoon. In contrast, winter has the lowest CV values throughout the day, consistently remaining below 0.04, reflecting minimal ventilation needs during this season.

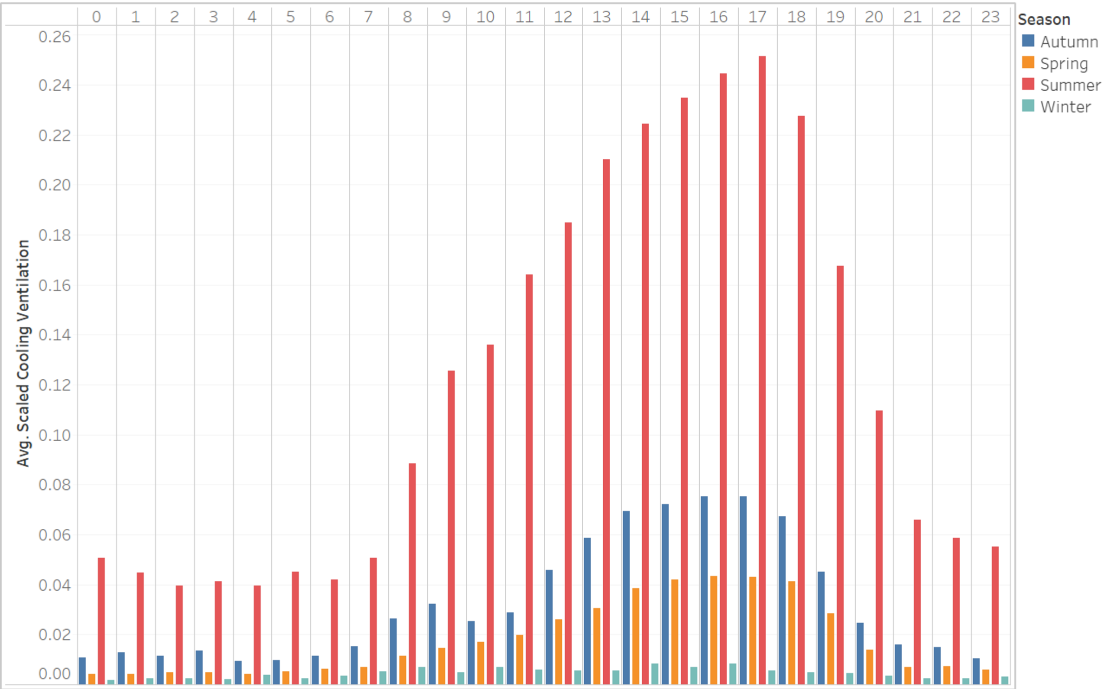

Figure 4. Average of Scaled CV for each Season Hour

The average availability of FC exhibits distinct seasonal patterns throughout the day (Figure 5). Winter offers the highest average FC, with a notable peak between noon and 6 PM. This coincides with lower winter ambient temperatures, making FC more effective. In contrast, summer has the lowest FC availability due to higher ambient temperatures that limit its cooling potential. Autumn and spring show moderate FC levels, with increases observed during midday and early afternoon hours.

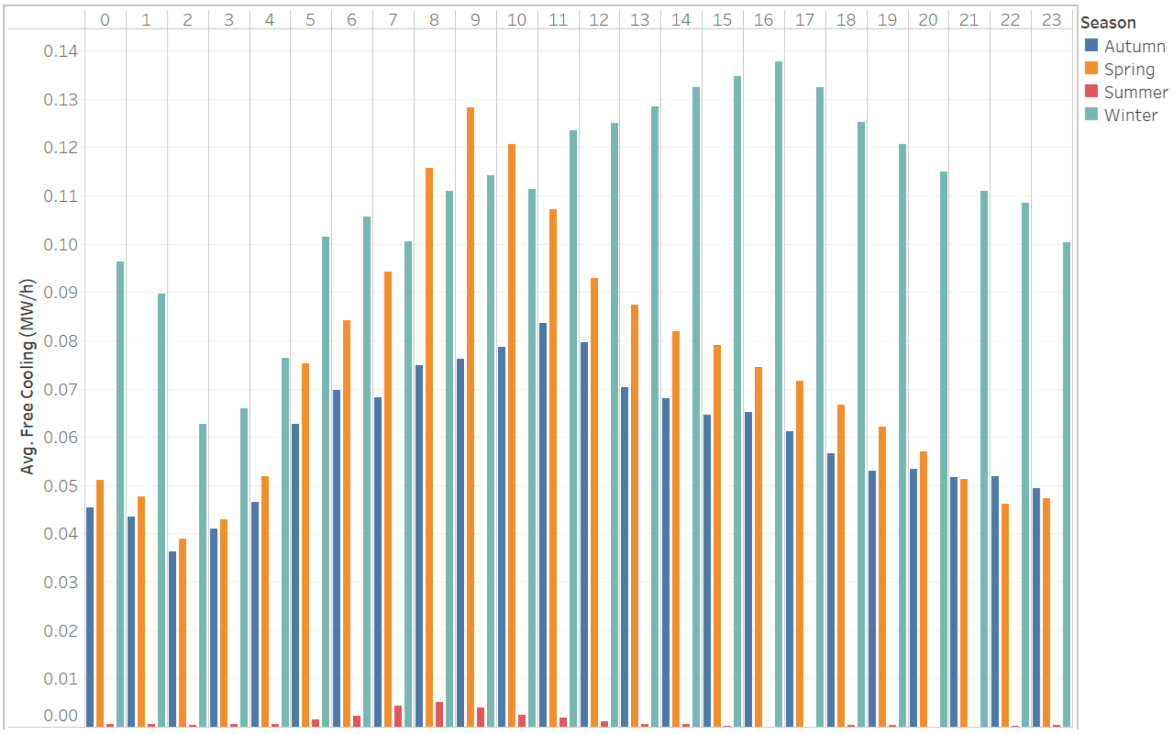

Figure 5. The average of Scaled FC for each season is broken down by hour

3-5- Features

The cooling consumption dataset contains key meteorological variables essential for analyzing and predicting building cooling energy use. These variables are obtained from multiple weather stations surrounding the building of interest. Typically, these variables include air temperature, relative humidity, wind speed, and precipitation levels.

While all stations measure these core variables, slight discrepancies may arise due to variations in station location and microclimates. For instance, a station near a body of water or within a built-up area might record higher wind speed or humidity than others. Despite these potential variations, including these essential variables from multiple stations strengthens the overall dataset. This comprehensive data collection enhances the reliability and detail of the information available for cooling consumption analysis and prediction.

3-5-1- Features Division

This study aims to predict a building's cooling needs, encompassing CC, CV, FC, and TC requirements. We will leverage data from various weather stations and analyze it using three feature groups (3, 7, and all features) based on their correlation with cooling needs (refer to Table 2 for detailed results).

Table 2 illustrates the correlations between weather station data and CC consumption. These correlations highlight key factors influencing cooling needs. At the BWS station, air temperature exhibits the strongest correlation (0.797781), indicating its primary influence on CC consumption, followed by relative humidity (0.590161) and global radiation (0.440239). In contrast, for stations 7341, 1420, and 1424, the hour of the day displays a consistently strong correlation (0.223645), suggesting its importance as a temporal factor for CC. Additionally, relative humidity exhibits notable correlations across all stations, ranging from 0.111117 to 0.127720, underlining its consistent influence on cooling needs.

Like cooling consumption, we analyze weather data to identify critical factors influencing FC. Table 3 details the correlations between weather station data and FC availability.

The analysis reveals that the month of the year exhibits the strongest correlation across all stations (0.178541), suggesting a significant influence of seasonal changes on FC opportunities. At the BWS station, air temperature shows the highest correlation (0.628743), indicating its primary influence on FC potential. Additionally, relative humidity displays notable correlations across all stations, with a robust correlation at BWS (0.301435), highlighting its impact on FC efficiency. Finally, the season exhibits a consistent influence, especially at stations 7341 (0.113830) and 1424 (0.113830), underlining the importance of seasonal variations in FC prediction.

Table 2. Correlation of CC Consumptions Features

Variable	Correlation	Variable	Correlation	Variable	Correlation	Variable	Correlation
7341		**1420**		**BWS**		**1424**	
Hour	0.223645	Hour	0.223645	Air Temperature	0.797781	Hour	0.223645
Relative Humidity	0.127720	Relative Humidity	0.115350	Relative Humidity	0.590161	Relative Humidity	0.111117
Month	0.085430	Sunshine Duration	0.094734	Global Radiation	0.440239	Month	0.085430
Highest Wind Peak	0.084294	Month	0.085430	Brightness Highest Value	0.397482	Year	0.076389
Visibility	0.081090	Year	0.076389	Hour	0.223645	Air Pressure	0.059030
Year	0.076389	Wind Speed	0.070061	Wind Speed	0.212208	Air Temperature	0.058339
Air Temperature	0.068770	Dew Point	0.067123	Month	0.085430	Wet Bulb	0.028411
Wind Speed	0.064732	Air Temperature	0.065112	Year	0.076389	Absolute Humidity	0.023573
Humidity Temperature	0.036879	Visibility	0.062663	Wind Direction	0.067432	Day	0.023194
Wind Direction	0.028841	Wind Direction	0.055273	Precipitation (Yes/No)	0.050850	Weekday	0.022532
Observed Weather	0.024922	Humidity Temperature	0.034361	Amount of Precipitation	0.028002	Vapor Pressure	0.018746
Day	0.023194	Absolute Humidity	0.026353	Day	0.023194	Dew Point	0.013562
Cloud Coverage	0.022879	Air Pressure	0.023387	Weekday	0.022532	Season	0.010300
Weekday	0.022532	Day	0.023194	Air Pressure	0.012489	Precipitation (Yes/No)	0.007889
Absolute Humidity	0.017155	Weekday	0.022532	Season	0.010300	Precipitation	0.006165
Precipitation (Yes/No)	0.014584	Vapor Pressure	0.021025	Precipitation	0.001209		
Air Pressure	0.012452	Season	0.010300				
Vapor Pressure	0.012168	Observed Weather	0.003400				
Season	0.010300	Precipitation (Yes/No)	0.000205				
Dew Point	0.005185	Precipitation	0.000126				
Precipitation Height	0.000050						

Table 3. Correlation of FC Consumptions Features

Variable	Correlation	Variable	Correlation	Variable	Correlation	Variable	Correlation
7341		1420		BWS		1424	
Month	0.178541	Month	0.178541	Air Temperature	0.628743	Month	0.178541
Season	0.113830	Season	0.113830	Relative Humidity	0.301435	Season	0.113830
Year	0.109299	Year	0.109299	Month	0.178541	Year	0.109299
Relative Humidity	0.097668	Sunshine Duration	0.108008	Wind Speed	0.130151	Relative Humidity	0.086421
Air Temperature	0.082186	Relative Humidity	0.094551	Global Radiation	0.115437	Air Pressure	0.083411
Wind Speed	0.055798	Air Temperature	0.080636	Season	0.113830	Air Temperature	0.077192
Highest Wind Peak	0.053361	Dew Point	0.078443	Year	0.109299	Wet Bulb	0.054578
Humidity Temperature	0.051801	Humidity Temperature	0.058192	Brightness Highest Value	0.078309	Hour	0.041579
Hour	0.041579	Wind Speed	0.046073	Hour	0.041579	Day	0.028216
Visibility	0.031385	Hour	0.041579	Day	0.028216	Vapor Pressure	0.027312
Day	0.028216	Day	0.028216	Wind Direction	0.026914	Dew Point	0.025530
Vapor Pressure	0.024235	Wind Direction	0.028169	Air Pressure	0.023500	Absolute Humidity	0.023315
Observed Weather	0.023241	Observed Weather	0.026265	Weekday	0.017090	Weekday	0.017090
Dew Point	0.021579	Vapor Pressure	0.023900	Precipitation	0.008962	Precipitation	0.007501
Absolute Humidity	0.019922	Absolute Humidity	0.019538	Precipitation (Yes/No)	0.005564	Precipitation (Yes/No)	0.004595
Cloud Coverage	0.017990	Weekday	0.017090	Amount of Precipitation	0.000293		
Weekday	0.017090	Precipitation	0.009951				
Wind Direction	0.013439	Visibility	0.009411				
Precipitation (Yes/No)	0.010599	Precipitation (Yes/No)	0.002358				
Precipitation Height	0.001926	Air Pressure	0.001280				
Air Pressure	0.001543						

Table 4 presents the correlations between weather station data and CV requirements. The analysis identifies Global Radiation and Air Temperature as the two most significant variables influencing CV.

Global radiation exhibits a strong positive correlation (0.438349) with CV, suggesting a direct relationship between solar energy and CV needs. Higher levels of solar radiation lead to increased interior temperature, consequently driving up CV requirements. Similarly, air temperature displays a significant positive correlation (0.043090) with CV. Warmer ambient temperatures necessitate extensive cooling efforts to maintain comfortable indoor conditions, resulting in higher CV requirements.

Table 4. Correlation of CV Consumptions Features

Variable	Correlation	Variable	Correlation	Variable	Correlation	Variable	Correlation
7341		1420		BWS		1424	
Hour	0.147195	Sunshine Duration	0.134351	Global Radiation	0.438349	Relative Humidity	0.120758
Highest Wind Peak	0.116541	Relative Humidity	0.131388	Relative Humidity	0.390939	Month	0.094191
Wind Speed	0.105239	Month	0.094191	Brightness Highest Value	0.370621	Year	0.083054
Month	0.094191	Wind Speed	0.093683	Wind Speed	0.153121	Absolute Humidity	0.049671
Year	0.083054	Year	0.083054	Hour	0.147195	Air Pressure	0.045492
Visibility	0.077518	Dew Point	0.056454	Month	0.094191	Vapor Pressure	0.043962
Air Temperature	0.058446	Air Temperature	0.053507	Year	0.083054	Air Temperature	0.043090
Absolute Humidity	0.042722	Wind Direction	0.053047	Precipitation Yes/No	0.029594	Dew Point	0.040656
Vapor Pressure	0.036438	Absolute Humidity	0.052098	Season	0.025401	Season	0.025401
Wind Direction	0.033666	Vapor Pressure	0.045722	Weekday	0.019418	Weekday	0.019418
Dew Point	0.030622	Visibility	0.045410	Wind Direction	0.015905	Day	0.012612
Season	0.025401	Season	0.025401	Day	0.012612	Precipitation Yes/No	0.009450
Observed Weather	0.022366	Weekday	0.019418	Air Pressure	0.010185	Wet Bulb	0.007731
Precipitation Yes/No	0.021265	Precipitation	0.014825	Precipitation	0.010014	Precipitation	0.004275
Humidity Temperature	0.020933	Humidity Temperature	0.014793	Amount Precipitation	0.001973		
Weekday	0.019418	Air Pressure	0.013387				
Air Pressure	0.013098	Day	0.012612				
Day	0.012612	Precipitation Yes/No	0.010181				
Coverage Clouds	0.011996	Observed Weather	0.001528				
Precipitation Height	0.004373						

Finally, similar to CC, FC, and CV, we examine weather data to identify critical factors influencing TC needs. Table 5 details the correlations between weather station data and TC consumption.

The analysis reveals that the hour of the day is a consistently important factor across most stations, exhibiting the strongest correlation (0.208693) at stations 7341, 1420, and 1424. This highlights the temporal influence on TC requirements. At the BWS station, air temperature has the strongest correlation (0.774650), indicating its primary influence on TC needs. The relative humidity is also a critical variable, with significant correlations observed at BWS (0.550218) and station 7341 (0.144503), underlining its impact on overall cooling consumption. Furthermore, solar-related factors play a role, as evidenced by the correlations with sunshine duration (0.116026 at 1420) and global radiation (0.469275 at BWS).

4- Research Methodology

This study leverages a comprehensive methodology that emphasizes the importance of localized weather data in improving the accuracy of cooling consumption prediction models (Figure 6). We adopt a systematic approach, incorporating various ML models, including K-Nearest Neighbor (KNN), Decision Tree (DT), Support Vector Regression (SVR), and Linear Regression (LR). Ensemble learning models such as RF, GB, XGBoost, and Adaboost are employed. Additionally, DL models including LSTM and GRU are explored. The performance of these models is evaluated using a suite of metrics, including Mean Squared Error (MSE), Mean Absolute Error (MAE), Root Mean Squared Error (RMSE), Mean Absolute Percentage Error (MAPE), and R-squared (R^2).

4-1- Pre-Processing

The data preprocessing stage starts by separating numeric columns from non-numeric ones. Columns representing 'Year', 'Month', and 'Hour' are excluded during this process. Missing value imputation follows a hierarchical approach, prioritizing group means based on increasingly finer categories: first by 'Year,' 'Month,' and 'Hour'; then by 'Year' and 'Month'; and finally by 'Year' and 'Season.' Any remaining missing values are imputed using the annual average. Lastly, label encoding converts categorical variables such as 'Season' and 'Weekday' into numerical features.

Table 5. Correlation of TC Consumptions Features

Variable	Correlation	Variable	Correlation	Variable	Correlation	Variable	Correlation
7341		**1420**		**BWS**		**1424**	
Hour	0.208693	Hour	0.208693	Air Temperature	0.774650	Hour	0.208693
Relative Humidity	0.144503	Relative Humidity	0.129246	Relative Humidity	0.550218	Relative Humidity	0.122153
Highest Wind Peak	0.103823	Sunshine Duration	0.116026	Global Radiation	0.469275	Month	0.095327
Month	0.095327	Month	0.095327	Brightness Highest Value	0.414061	Year	0.083389
Wind Speed	0.086205	Wind Speed	0.085344	Hour	0.208693	Air Pressure	0.057925
Visibility	0.085585	Year	0.083389	Wind Speed	0.203818	Air Temperature	0.054612
Year	0.083389	Dew Point	0.065850	Month	0.095327	Absolute Humidity	0.037467
Air Temperature	0.067838	Air Temperature	0.063372	Year	0.083389	Vapor Pressure	0.032004
Wind Direction	0.033614	Wind Direction	0.059498	Wind Direction	0.051911	Dew Point	0.027041
Humidity Temperature	0.031442	Visibility	0.059413	Precipitation (Yes/No)	0.045673	Weekday	0.023102
Absolute Humidity	0.030313	Absolute Humidity	0.040382	Weekday	0.023102	Wet Bulb	0.020378
Observed Weather	0.025067	Vapor Pressure	0.034323	Day	0.020063	Day	0.020063
Vapor Pressure	0.024512	Humidity Temperature	0.027176	Amount of Precipitation	0.017516	Precipitation (Yes/No)	0.008838
Weekday	0.023102	Weekday	0.023102	Air Pressure	0.011698	Precipitation	0.005629
Cloud Coverage	0.021020	Air Pressure	0.020776	Precipitation	0.003429	Season	0.003266
Day	0.020063	Day	0.020063	Season	0.003266		
Precipitation (Yes/No)	0.018822	Precipitation	0.006065				
Dew Point	0.017346	Precipitation (Yes/No)	0.004509				
Air Pressure	0.013444	Season	0.003266				
Season	0.003266	Observed Weather	0.002234				
Precipitation Height	0.001645						

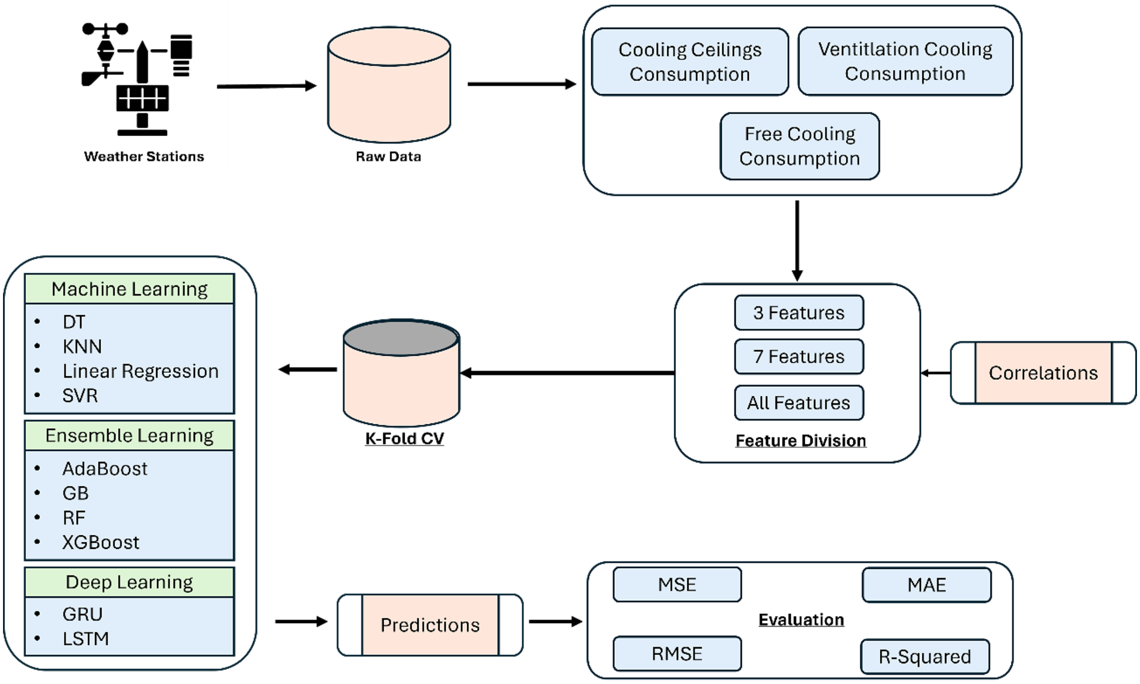

Figure 6. Proposed Methodology

4-2- Modeling

The study evaluates various models, including KNN, SVR, DT, LR, RF, GB, AdaBoost, LSTM, and GRU, to determine the impact of localized weather data on the accuracy of predictive models for cooling consumption. Details of these models are listed in Table 6.

Table 6. Details of Models

Model	Working Mechanism	Advantage(s)	Limitation(s)	Scalability
		Machine Learning		
KNN [35]	Non-parametric, instance-based	Utilizes localized weather data for accurate predictions	Sensitive to noisy or irrelevant features	Limited scalability, as it requires storing all training data
SVR [36]	It uses support vectors to define a hyperplane	Effective with complex data and high-dimensional spaces	Computationally intensive and sensitive to kernel choice	Moderate scalability may become slow with large datasets
DT [37]	Makes decisions based on feature values	Interpretable and easy to visualize	Prone to overfitting, especially with complex data	Moderate scalability can manage large datasets but prone to overfitting
LR [38]	Models' linear relationship between variables	Simple and easy to implement	Assumes a linear relationship between variables	Highly scalable, efficient for large datasets
		Ensemble Learning		
XGBoost [39]	Sequentially adding DT to correct errors made by previous trees	exhibits high predictive accuracy and efficiency	susceptibility to overfitting, especially when dealing with noisy data or shallow trees.	Capable of handling large datasets efficiently due to its parallel and distributed computing capabilities
RF [40]	Ensemble of DT	Oversees high-dimensional data well and is resistant to overfitting	Complexity increases with the number of trees	Moderate scalability, can manage large datasets but slower training with many trees.
GB [41]	Sequentially builds multiple weak learners	Provides high predictive accuracy	Prone to overfitting and can be computationally expensive	Moderate scalability, slower than RF due to sequential training
AdaBoost [42]	Ensemble method using a series of weak classifiers	Robust against overfitting and performs well with diverse data	Sensitive to noisy data and outliers	Moderate scalability, can handle large datasets but slower training with many weak learners.
		DL		
LSTM [43]	Recurrent neural network for sequence prediction	Effective for modeling time-series data	Computationally intensive and may suffer from vanishing gradients	Limited scalability, slow training, and inference with large sequences
GRU [44]	A simplified version of LSTM, efficient for training	Balances model complexity and performance	It may not capture long-term dependencies as effectively as LSTM	Moderate scalability, faster training, and inference compared to LSTM

4-3- Evaluation Metrics

The study employs MSE, MAE, RMSE and R^2 to evaluate model performance, standard metrics for assessing predictive accuracy. Additionally, incorporating these metrics to evaluate model stability and sensitivity, such as prediction interval coverage probability or calibration plots, could enhance understanding of the model's reliability and its ability to generalize across different conditions. The summary of these metrics is represented in Table 7.

Table 7. **Details of Evaluation Metrics**

Metric	Description	Equation	Criteria
Mean Squared Error (MSE) [45]	Measures the average squared difference between predicted and actual values	$MSE: \frac{1}{n}\sum_{i=1}^{n}(y_i - \hat{y}_i)^2$	Lower values indicate better model performance
Mean Absolute Error (MAE) [46]	Measures the average absolute difference between predicted and actual values	$MAE: \frac{1}{n}\sum_{i=1}^{n}\lvert y_i - \hat{y}_i\rvert^2$	lower values indicating better model performance.
Root Mean Squared Error (RMSE) [47]	Measures the square root of the average squared difference between predicted and actual values	$RMSE: \sqrt{\frac{1}{n}\sum_{i=1}^{n}(y_i - \hat{y}_i)^2}$	Lower values indicate better model performance
R-squared (R^2) [48]	Measures the proportion of the variance in the dependent variable that is predictable from the independent variables	$R^2 = 1 - \frac{\frac{1}{n}\sum_{i=1}^{n}(y_i - \hat{y}_i)^2}{\frac{1}{n}\sum_{i=1}^{n}(y_i - \bar{y})^2}$	Higher values (close to 1) indicate better model performance

4-4- Experimental Setup

In this research, popular Python libraries were used throughout various stages. Pandas facilitates data manipulation and analysis, while NumPy underpins numerical computations and array operations. Scikit-learn provides a comprehensive suite of ML algorithms for model training, evaluation, and preprocessing tasks. DL models are implemented using TensorFlow or PyTorch, offering high-level APIs for building and optimizing neural networks. Data visualization is performed using Matplotlib to gain insights into dataset characteristics and monitor model performance.

To ensure reproducibility, experiments employ consistent random seed values. The dataset is split into an 80% training set and a 20% testing set for model evaluation. K-fold cross-validation with K=5 is utilized during training to mitigate overfitting and assess model generalizability. Various experiments are conducted, exploring different feature sets, as detailed in Table 8.

Table 8. **Summary of Experimentation**

Features	CC	FC	TC	CV
		1420		
3-Features	Hour, Relative Humidity, Sunshine Duration	Month, Season, Year	Hour, Relative Humidity, Sunshine Duration	Sunshine Duration, Relative Humidity Month
7-Features	Hour, Relative Humidity, Sunshine Duration, Month, Year, Wind Speed, Dew Point	Month, Season, Year, Sunshine Duration, Relative Humidity, Air Temperature, Dew Point	Hour, Relative Humidity, Sunshine Duration, Month, Wind Speed, Year, Dew Point	Sunshine Duration, Relative Humidity, Month, Wind Speed, Year, Dew Point, Air Temperature
All	All the features included in Table 2	All the features included in Table 3	All the features included in Table 4	Included in Table 5
		1424		
3-Features	Air Temperature, Relative Humidity, Global Radiation	Month, Season, Year	Hour, Relative Humidity, Month,	Relative Humidity, Month, Year
7-Features	Hour, Relative Humidity, Month, Year, Air Pressure, Air Temperature, Wet Bulb	Month, Season, Year, Relative Humidity, Air Pressure, Air Temperature, Wet Bulb	Hour, Relative Humidity, Month, Year, Air Pressure, Air Temperature, Wet Bulb	Relative Humidity, Month, Year, Absolute Humidity, Air Pressure, Vapor Pressure, Air Temperature
All	All the features included in Table 2	All the features included in Table 3	All the features included in Table 4	Included in Table 5
		7341		
3-Features	Hour, Relative Humidity, Month	Month, Season, Year	Hour, Relative Humidity, Highest Wind Peak	Hour, Highest Wind Peak, Wind Speed
7-Features	Hour, Relative Humidity Month, Highest Wind Peak, Visibility, Year, Air Temperature	Month, Season, Year, Relative Humidity, Air Temperature, Wind Speed, Highest Wind Peak	Hour, Relative Humidity, Highest Wind Peak, Month Wind Speed, Visibility, Year	Hour, Highest Wind Peak, Wind Speed, Month, Year, Visibility, Air Temperature
All	All the features included in Table 2	All the features included in Table 3	All the features included in Table 4	All the features included in Table 5
		BWS		
3-Features	Air Temperature, Relative Humidity, Global Radiation	Air Temperature, Relative Humidity, Month	Air Temperature, Relative Humidity, Global Radiation	Global Radiation, Relative Humidity, Brightness Highest Value
7-Features	Air Temperature, Relative Humidity, Global Radiation, Brightness Highest Value, Hour, Wind Speed, Month	Air Temperature, Relative Humidity, Month, Wind Speed, Global Radiation, Season, Year	Air Temperature, Relative Humidity, Global Radiation, Brightness Highest Value, Hour, Wind Speed, Month	Hour, Highest Wind Peak, Wind Speed, Month, Year, Visibility, Air Temperature
All	All the features included in Table 2	All the features included in Table 3	All the features included in Table 4	All the features included in Table 5

5- Results and Discussion

The results section analyzes the performance of various ML, ensemble learning, and DL models in predicting CC, TC, FC, and CV for weather stations 1420, 1424, 7341, and BWS. The analysis considers different feature sets to assess model generalizability. Model performance is evaluated using a suite of metrics, including MSE, MAE, RMSE, and R^2. These metrics provide insights into the models' accuracy and predictive power across diverse datasets and feature combinations.

5-1- Cooling Ceiling

This section explores the performance of various models across different weather stations and feature sets.

Concerning Station 1420, KNN emerged as the strongest performer among the considered ML models, particularly with all features included (MSE: 0.013, MAE: 0.064, RMSE: 0.114, R^2: 0.763). Notably, performance improved with an increase in features. In the ensemble learning category, RF achieved the top performance (MSE: 0.005, MAE: 0.035, RMSE: 0.067, R^2: 0.917), indicating high accuracy and reliability. This strong performance by RF was consistent for station 1424 as well (MSE: 0.004, MAE: 0.033, RMSE: 0.065, R^2: 0.924). LSTM networks, representing the deep learning category, achieved moderate results with 3 features (MSE: 0.050, MAE: 0.183, RMSE: 0.224, R^2: 0.078). However, the performance showed a slight decline when using all features (MSE: 0.026, MAE: 0.108, RMSE: 0.160, R^2: 0.528). Station 1424 also decreased performance with LSTMs using all features (MSE: 0.024, MAE: 0.105, RMSE: 0.156, R^2: 0.553), suggesting a need for further optimization (refer to Table 9 for detailed results).

Concerning Station 7341, the best-performing ML model was DT with all features included (MSE: 0.010, MAE: 0.045, RMSE: 0.099, R^2: 0.820) (refer to Table 10 for details). Like station 1420, RF excelled in the ensemble learning category (MSE: 0.005, MAE: 0.036, RMSE: 0.069, R^2: 0.912). LSTM networks in the deep learning category delivered satisfactory results with 3 features (MSE: 0.019, MAE: 0.089, RMSE: 0.137, R^2: 0.655). However, performance dropped when using all features.

At station BWS, KNN performed well among the ML models (MSE: 0.008, MAE: 0.046, RMSE: 0.088, R^2: 0.857). GB achieved the best results in the ensemble learning category (MSE: 0.007, MAE: 0.050, RMSE: 0.085, R^2: 0.868). However, RF also exhibited strong performance (MSE: 0.004, MAE: 0.034, RMSE: 0.064, R^2: 0.926). LSTM networks, representing deep learning, delivered notable results with 5 features (MSE: 0.011, MAE: 0.064, RMSE: 0.106, R^2: 0.794).

It is evident from the results of CC prediction that KNN excelled at Station 1420 due to its ability to effectively capture local data patterns, which improved with an increase in features. RF consistently outperformed others in the ensemble learning category because of its robustness in managing high-dimensional data and mitigating overfitting through averaging multiple DTs, which enhanced accuracy and reliability. For instance, at Station 7341, RF's capability to aggregate diverse decision boundaries allowed it to adapt to complex data structures better than individual models like DT. In contrast, LSTM networks, designed to capture temporal dependencies, showed moderate results, indicating that while they can model sequential data, they may require further optimization to handle the intricacies of cooling load prediction with all features included.

Table 9. Evaluation of Models on 1420 and 1424 Weather Station Dataset in CC Prediction

1420												
	3-Features				5-Features				All-Features			
Algorithm	**MSE**	**MAE**	**RMSE**	**R^2**	**MSE**	**MAE**	**RMSE**	**R^2**	**MSE**	**MAE**	**RMSE**	**R^2**
ML												
KNN	0.058	0.183	0.241	-0.067	0.014	0.069	0.117	0.747	0.013	0.064	0.114	0.763
SVR	0.056	0.174	0.237	-0.030	0.018	0.097	0.132	0.678	0.013	0.085	0.114	0.763
DT	0.075	0.192	0.274	-0.379	0.022	0.075	0.148	0.598	0.009	0.042	0.093	0.842
LR	0.051	0.182	0.227	0.057	0.051	0.180	0.225	0.068	0.051	0.180	0.225	0.071
Ensemble Learning												
XGBoost	0.051	0.174	0.226	0.062	0.013	0.071	0.113	0.767	0.006	0.049	0.077	0.892
RF	0.057	0.179	0.239	-0.048	0.011	0.060	0.105	0.799	0.005	0.035	0.067	0.917
GB	0.049	0.177	0.222	0.095	0.016	0.081	0.125	0.714	0.013	0.078	0.115	0.755
AdaBoost	0.055	0.197	0.234	-0.007	0.022	0.117	0.149	0.595	0.024	0.125	0.156	0.551
DL												
LSTM	0.050	0.183	0.224	0.078	0.018	0.088	0.133	0.673	0.026	0.108	0.160	0.528
GRU	0.051	0.179	0.226	0.065	0.018	0.090	0.133	0.675	0.016	0.079	0.126	0.710

1424												
	3-Features				5-Features				All-Features			
Algorithm	**MSE**	**MAE**	**RMSE**	**R^2**	**MSE**	**MAE**	**RMSE**	**R^2**	**MSE**	**MAE**	**RMSE**	**R^2**
ML												
KNN	0.021	0.086	0.146	0.610	0.012	0.063	0.111	0.773	0.009	0.050	0.095	0.833
SVR	0.020	0.101	0.142	0.629	0.017	0.096	0.132	0.682	0.013	0.082	0.113	0.766
DT	0.031	0.101	0.177	0.424	0.019	0.068	0.137	0.656	0.008	0.040	0.091	0.849
LR	0.051	0.181	0.226	0.060	0.051	0.181	0.225	0.067	0.051	0.181	0.225	0.067
Ensemble Learning												
XGBoost	0.019	0.085	0.138	0.648	0.012	0.068	0.108	0.786	0.006	0.047	0.075	0.895
RF	0.024	0.091	0.154	0.563	0.010	0.055	0.100	0.818	0.004	0.033	0.065	0.924
GB	0.018	0.085	0.134	0.670	0.016	0.081	0.125	0.714	0.013	0.078	0.115	0.759
AdaBoost	0.021	0.097	0.146	0.609	0.020	0.101	0.141	0.637	0.021	0.108	0.145	0.613
DL												
LSTM	0.019	0.087	0.138	0.652	0.018	0.086	0.133	0.675	0.024	0.105	0.156	0.553
GRU	0.020	0.091	0.141	0.635	0.017	0.087	0.130	0.687	0.014	0.079	0.120	0.736

Table 10. Evaluation of Models on 7341 and BWS Weather Station dataset in CC Prediction

7341												
	3-Features				5-Features				All-Features			
Algorithm	**MSE**	**MAE**	**RMSE**	**R^2**	**MSE**	**MAE**	**RMSE**	**R^2**	**MSE**	**MAE**	**RMSE**	**R^2**
ML												
KNN	0.020	0.085	0.143	0.625	0.015	0.071	0.122	0.727	0.015	0.071	0.121	0.730
SVR	0.020	0.101	0.142	0.629	0.018	0.097	0.133	0.675	0.014	0.088	0.118	0.745
DT	0.031	0.101	0.176	0.430	0.021	0.071	0.143	0.623	0.010	0.045	0.099	0.820
LR	0.051	0.180	0.226	0.061	0.051	0.181	0.226	0.066	0.051	0.180	0.225	0.069
Ensemble Learning												
XGBoost	0.018	0.083	0.136	0.662	0.012	0.071	0.111	0.774	0.006	0.051	0.079	0.886
RF	0.023	0.090	0.151	0.580	0.010	0.057	0.101	0.812	0.005	0.036	0.069	0.912
GB	0.018	0.085	0.134	0.670	0.016	0.082	0.126	0.710	0.013	0.078	0.115	0.756
AdaBoost	0.021	0.095	0.144	0.618	0.020	0.101	0.141	0.633	0.022	0.113	0.148	0.595
DL												
LSTM	0.019	0.089	0.137	0.655	0.018	0.088	0.133	0.676	0.029	0.122	0.171	0.463
GRU	0.019	0.089	0.139	0.644	0.018	0.089	0.134	0.668	0.016	0.080	0.125	0.712
BWS												
Algorithm	**MSE**	**MAE**	**RMSE**	**R^2**	**MSE**	**MAE**	**RMSE**	**R^2**	**MSE**	**MAE**	**RMSE**	**R^2**
ML												
KNN	0.014	0.063	0.116	0.751	0.011	0.054	0.104	0.803	0.008	0.046	0.088	0.857
SVR	0.014	0.086	0.117	0.750	0.011	0.069	0.103	0.806	0.008	0.063	0.090	0.852
DT	0.018	0.102	0.135	0.665	0.016	0.062	0.127	0.706	0.008	0.042	0.090	0.852
LR	0.022	0.079	0.149	0.593	0.018	0.099	0.132	0.678	0.016	0.094	0.127	0.703
Ensemble Learning												
XGBoost	0.012	0.061	0.111	0.774	0.008	0.047	0.091	0.847	0.004	0.032	0.063	0.926
RF	0.013	0.062	0.113	0.765	0.009	0.051	0.096	0.831	0.004	0.034	0.064	0.926
GB	0.011	0.058	0.106	0.794	0.009	0.053	0.097	0.827	0.007	0.050	0.085	0.868
AdaBoost	0.015	0.078	0.123	0.723	0.021	0.125	0.146	0.611	0.014	0.079	0.117	0.749
DL												
LSTM	0.013	0.066	0.112	0.770	0.011	0.064	0.106	0.794	0.012	0.072	0.111	0.775
GRU	0.013	0.068	0.113	0.765	0.011	0.064	0.104	0.802	0.013	0.078	0.113	0.767

5-2- Total Cooling

XGBoost excelled at predicting TC loads across all weather stations (1420, 1424, 7341, and BWS) and feature sets, demonstrating its robustness and reliability (refer to Tables 11 and 12 for detailed results).

Concerning Station 1420 and 1424, XGBoost consistently achieved top performance, particularly with all features included. For example, station 1424 achieved an MSE of 0.009, MAE of 0.056, RMSE of 0.096, and an R^2 of 0.925, showcasing exceptional accuracy. Focusing on Station 7341 and similar to other stations, XGBoost dominated, achieving high accuracy with all features (MSE: 0.011, MAE: 0.060, RMSE: 0.104, R^2: 0.911). RF also performed well, particularly with all features (MSE: 0.013, MAE: 0.073, RMSE: 0.113, R^2: 0.894). Moving to Station BWS, XGBoost maintained its dominance, achieving remarkable accuracy with all features (MSE: 0.007, MAE: 0.051, RMSE: 0.085, R^2: 0.941). RF again exhibited competitive performance across various feature sets.

XGBoost's exceptional performance in predicting TC loads across all weather stations can be attributed to its ability to handle high-dimensional data and model complex relationships through GB techniques. Its robustness and reliability stem from its iterative approach of combining weak learners to form a robust predictive model, effectively reducing bias and variance. Additionally, XGBoost's capability to select features and handle missing data ensures high accuracy, as seen in its consistently top performance metrics. In contrast, while RF also performed well due to its ensemble nature, it was slightly less effective than XGBoost in capturing intricate data patterns. DL models like LSTM and GRU, although promising with fewer features, struggled with the complexity of all features, indicating their need for more sophisticated optimization and feature selection strategies to achieve similar levels of accuracy.

Table 11. Evaluation of Models on 1420 and 1424 Weather Station dataset in TC Prediction

1420												
	3-Features				5-Features				All-Features			
Algorithm	**MSE**	**MAE**	**RMSE**	**R^2**	**MSE**	**MAE**	**RMSE**	**R^2**	**MSE**	**MAE**	**RMSE**	**R^2**
ML												
KNN	0.116	0.253	0.340	0.053	0.032	0.104	0.180	0.735	0.020	0.074	0.141	0.836
SVR	0.128	0.231	0.357	-0.046	0.044	0.135	0.209	0.643	0.029	0.098	0.170	0.764
DT	0.129	0.257	0.359	-0.054	0.048	0.114	0.219	0.607	0.032	0.118	0.178	0.739
LR	0.170	0.272	0.413	-0.395	0.113	0.250	0.337	0.070	0.113	0.250	0.336	0.075
Ensemble Learning												
XGBoost	0.110	0.245	0.331	0.101	0.026	0.094	0.162	0.785	0.010	0.058	0.098	0.922
RF	0.114	0.243	0.338	0.063	0.031	0.108	0.175	0.749	0.012	0.072	0.110	0.901
GB	0.129	0.253	0.359	-0.055	0.038	0.121	0.195	0.689	0.032	0.116	0.178	0.740
AdaBoost	0.133	0.291	0.364	-0.087	0.048	0.154	0.220	0.603	0.058	0.187	0.240	0.526
DL												
LSTM	0.110	0.249	0.332	0.095	0.041	0.126	0.203	0.662	0.062	0.156	0.248	0.495
GRU	0.110	0.247	0.332	0.096	0.041	0.123	0.203	0.661	0.033	0.115	0.183	0.726
1424												
	3-Features				5-Features				All-Features			
Algorithm	**MSE**	**MAE**	**RMSE**	**R^2**	**MSE**	**MAE**	**RMSE**	**R^2**	**MSE**	**MAE**	**RMSE**	**R^2**
ML												
KNN	0.047	0.136	0.216	0.617	0.029	0.096	0.170	0.764	0.019	0.078	0.139	0.841
SVR	0.050	0.130	0.224	0.590	0.042	0.134	0.205	0.654	0.031	0.115	0.175	0.749
DT	0.075	0.153	0.273	0.388	0.043	0.107	0.207	0.648	0.019	0.072	0.137	0.845
LR	0.115	0.251	0.339	0.057	0.114	0.251	0.338	0.066	0.114	0.250	0.337	0.069
Ensemble Learning												
XGBoost	0.043	0.126	0.207	0.650	0.024	0.088	0.155	0.802	0.009	0.056	0.096	0.925
RF	0.045	0.127	0.213	0.627	0.028	0.103	0.167	0.772	0.011	0.069	0.107	0.906
GB	0.055	0.157	0.235	0.549	0.038	0.122	0.194	0.692	0.032	0.116	0.178	0.741
AdaBoost	0.056	0.136	0.236	0.545	0.047	0.153	0.218	0.611	0.047	0.152	0.217	0.613
DL												
LSTM	0.044	0.130	0.211	0.635	0.040	0.125	0.200	0.673	0.064	0.167	0.253	0.474
GRU	0.045	0.132	0.211	0.634	0.038	0.126	0.195	0.689	0.028	0.111	0.167	0.772

5-3- Cooling Ventilation

The analysis of machine learning models for predicting CV reveals several vital findings (refer to Table 13 for detailed results). KNN performed well across datasets (1420 and 1424) and feature sets (3, 5, all features), achieving competitive MSE and RMSE values. Notably, it exhibited relatively high R-squared values in dataset 1420, suggesting a good fit to the data. Among ensemble learning methods, RF emerged as the top performer. It consistently achieved the lowest MSE and RMSE values across datasets and feature sets. This strong performance is further supported by high R-squared values, indicating both predictive solid power and an excellent fit for the data. RF's ability to handle complex data relationships likely contributes to its superior performance. LSTM and GRU models showed promising results. These models performed consistently well across datasets and feature sets, with competitive MSE and RMSE values. Additionally, both models achieved relatively high R-squared values, indicating their capability to capture underlying patterns in the data and make accurate predictions.

Table 12. Evaluation of Models on 7341 and BWS Weather Station dataset in TC Prediction

7341.000												
	3-Features				**5-Features**				**All-Features**			
Algorithm	**MSE**	**MAE**	**RMSE**	**R^2**	**MSE**	**MAE**	**RMSE**	**R^2**	**MSE**	**MAE**	**RMSE**	**R^2**
ML												
KNN	0.131	0.259	0.362	-0.073	0.042	0.120	0.204	0.658	0.033	0.108	0.182	0.727
SVR	0.127	0.231	0.356	-0.041	0.048	0.141	0.218	0.610	0.034	0.122	0.184	0.722
DT	0.217	0.307	0.466	-0.780	0.055	0.126	0.235	0.547	0.023	0.078	0.151	0.813
LR	0.115	0.253	0.340	0.053	0.114	0.251	0.337	0.067	0.113	0.251	0.336	0.073
Ensemble Learning												
XGBoost	0.130	0.262	0.361	-0.066	0.030	0.101	0.173	0.754	0.011	0.060	0.104	0.911
RF	0.118	0.251	0.344	0.033	0.033	0.112	0.181	0.731	0.013	0.073	0.113	0.894
GB	0.110	0.247	0.331	0.099	0.038	0.122	0.195	0.687	0.032	0.117	0.179	0.737
AdaBoost	0.130	0.288	0.361	-0.069	0.049	0.159	0.222	0.597	0.056	0.187	0.236	0.542
DL												
LSTM	0.111	0.244	0.333	0.094	0.048	0.143	0.218	0.609	0.057	0.158	0.238	0.536
GRU	0.111	0.244	0.334	0.088	0.041	0.122	0.203	0.663	0.034	0.114	0.184	0.723
BWS												
Algorithm	**MSE**	**MAE**	**RMSE**	**R^2**	**MSE**	**MAE**	**RMSE**	**R^2**	**MSE**	**MAE**	**RMSE**	**R^2**
ML												
KNN	0.029	0.093	0.170	0.764	0.025	0.085	0.159	0.793	0.016	0.072	0.128	0.865
SVR	0.028	0.114	0.167	0.770	0.024	0.096	0.154	0.805	0.015	0.081	0.124	0.874
DT	0.045	0.153	0.211	0.634	0.039	0.099	0.198	0.678	0.017	0.069	0.131	0.859
LR	0.049	0.118	0.221	0.601	0.043	0.149	0.208	0.647	0.039	0.141	0.199	0.677
Ensemble Learning												
XGBoost	0.025	0.089	0.158	0.796	0.020	0.076	0.141	0.838	0.007	0.051	0.085	0.941
RF	0.027	0.091	0.164	0.780	0.021	0.078	0.147	0.824	0.008	0.050	0.088	0.936
GB	0.029	0.092	0.169	0.765	0.022	0.082	0.149	0.817	0.013	0.070	0.116	0.890
AdaBoost	0.030	0.110	0.173	0.753	0.033	0.136	0.183	0.726	0.037	0.168	0.193	0.693
DL												
LSTM	0.028	0.095	0.169	0.767	0.025	0.093	0.158	0.795	0.023	0.096	0.151	0.814
GRU	0.027	0.097	0.164	0.778	0.024	0.091	0.156	0.801	0.026	0.115	0.161	0.817

Table 13. Evaluation of Models on 1420 and 1424 Weather Station dataset in CV Prediction

1420												
	3-Features				5-Features				All-Features			
Algorithm	**MSE**	**MAE**	**RMSE**	**R^2**	**MSE**	**MAE**	**RMSE**	**R^2**	**MSE**	**MAE**	**RMSE**	**R^2**
Machine Learning												
KNN	0.021	0.088	0.147	-0.063	0.009	0.049	0.092	0.579	0.007	0.047	0.086	0.633
SVR	0.021	0.105	0.146	-0.050	0.011	0.070	0.107	0.434	0.009	0.066	0.095	0.556
DT	0.030	0.096	0.173	-0.474	0.014	0.055	0.116	0.330	0.008	0.043	0.087	0.627
LR	0.019	0.085	0.140	0.036	0.019	0.084	0.138	0.058	0.019	0.084	0.137	0.066
Ensemble Learning												
XGBoost	0.020	0.085	0.140	0.029	0.008	0.051	0.092	0.584	0.004	0.039	0.064	0.797
RF	0.022	0.089	0.149	-0.098	0.007	0.046	0.085	0.641	0.004	0.034	0.061	0.818
GB	0.018	0.083	0.135	0.095	0.010	0.054	0.099	0.511	0.009	0.054	0.095	0.558
AdaBoost	0.028	0.123	0.166	-0.366	0.014	0.080	0.118	0.306	0.017	0.101	0.131	0.151
Deep Learning												
LSTM	0.018	0.082	0.135	0.093	0.011	0.061	0.107	0.437	0.014	0.068	0.117	0.323
GRU	0.037	0.115	0.191	-0.108	0.010	0.057	0.101	0.493	0.012	0.067	0.108	0.421
1424												
Algorithm	**MSE**	**MAE**	**RMSE**	**R^2**	**MSE**	**MAE**	**RMSE**	**R^2**	**MSE**	**MAE**	**RMSE**	**R^2**
Machine Learning												
KNN	0.012	0.057	0.110	0.402	0.008	0.045	0.087	0.625	0.006	0.041	0.076	0.712
SVR	0.013	0.075	0.113	0.364	0.011	0.067	0.105	0.451	0.009	0.064	0.094	0.560
DT	0.017	0.065	0.131	0.148	0.013	0.053	0.112	0.376	0.007	0.041	0.083	0.660
LR	0.019	0.085	0.140	0.036	0.019	0.085	0.139	0.048	0.019	0.084	0.138	0.056
Ensemble Learning												
XGBoost	0.011	0.056	0.106	0.449	0.008	0.050	0.089	0.611	0.004	0.038	0.065	0.793
RF	0.013	0.059	0.116	0.339	0.007	0.044	0.083	0.662	0.003	0.033	0.058	0.832
GB	0.010	0.055	0.102	0.481	0.010	0.054	0.099	0.513	0.009	0.053	0.093	0.568
AdaBoost	0.013	0.068	0.113	0.372	0.018	0.102	0.135	0.102	0.014	0.087	0.119	0.294
Deep Learning												
LSTM	0.011	0.055	0.105	0.457	0.010	0.057	0.100	0.500	0.013	0.070	0.115	0.349
GRU	0.011	0.058	0.105	0.453	0.010	0.057	0.099	0.512	0.010	0.055	0.102	0.490

Focusing on weather stations 7341 and BWS (see to Table 14), the analysis of ensemble learning methods for CV prediction reveals the following: SVR emerged as the top performer across all feature sets for both stations. Consistent MSE, RMSE, and high R^2 values indicate its effectiveness in predicting CV, demonstrating robust predictive power with a good fit to the data. The DT algorithm also performed well, particularly in station 7341. Here, it showed promising results with lower MSE and RMSE values compared to other models. RF emerged as the best performing model with consistently lowest MSE, RMSE, and high R^2 values. This suggests superior prediction capabilities and good pattern recognition for CV across both stations. GB exhibited competitive performance, particularly in station 7341, with relatively low MSE and RMSE values.

Finally, the analysis of deep learning models for CV prediction in stations 7341 and BWS yielded promising results: both LSTM and GRU models demonstrated promising results. They consistently achieved low MSE and RMSE values across datasets, indicating their effectiveness in predicting CV. Furthermore, high R^2 values suggest their capability to capture complex patterns in the data and make accurate predictions.

The superior performance of RF in predicting CV can be attributed to its ensemble learning approach, which combines multiple decision trees to enhance predictive accuracy and handle complex data relationships effectively. RF's ability to manage high-dimensional datasets and mitigate overfitting through averaging the results of various trees contributes to its consistently low MSE and RMSE values, alongside high R^2 values, indicating a strong fit to the data. This robustness allows RF to capture intricate patterns and variability within the datasets, making it the top performer across multiple weather stations and feature sets. Its flexibility and strength in feature importance ranking also provide valuable insights, further solidifying its dominance in predictive modeling for CV.

5-4- Free Cooling

This section analysis the performance of the considered models for predicting FC loads across weather stations (1420, 1424, 7341, and BWS) and feature sets (refer to Table 15 and 16 for detailed results).

KNN emerged as the top performer among ML models for all stations when using all features. It achieved consistent performance with MSE around 0.002, MAE around 0.02, RMSE around 0.04, and R^2 around 0.6-0.7. XGBoost dominated the ensemble learning category across all stations and feature sets. It achieved superior performance with the lowest MSE (around 0.001), MAE (around 0.015), RMSE (around 0.028), and the highest R^2 (around 0.8) values, indicating strong accuracy and reliability in predicting FC loads. Finally, focusing on DL models, LSTM networks showed some promise, particularly with a moderate number of features (3 for stations 1424 and 7341, 5 for BWS). However, their performance generally declined when using all features, suggesting limitations in handling highly complex datasets. This highlights the need for further optimization techniques for LSTM models for FC prediction.

XGBoost's dominance in predicting FC loads across all weather stations and feature sets can be attributed to its robust ensemble learning mechanism, which combines the predictions of multiple weak learners to achieve high accuracy and reliability. Its ability to handle complex data relationships and prevent overfitting through regularization techniques contributes to its superior performance metrics, such as the lowest MSE, MAE, and RMSE values and the highest R^2 values. Additionally, XGBoost's efficiency in handling large datasets and feature interactions ensures strong predictive power, making it the most effective model for FC load prediction in this study.

Table 14. Evaluation of Models on 1420 and 1424 Weather Station dataset in CV Prediction

7341												
	3-Features				5-Features				All-Features			
Algorithm	**MSE**	**MAE**	**RMSE**	**R^2**	**MSE**	**MAE**	**RMSE**	**R^2**	**MSE**	**MAE**	**RMSE**	**R^2**
Machine Learning												
KNN	0.020	0.085	0.143	0.625	0.010	0.053	0.100	0.501	0.008	0.050	0.092	0.581
SVR	0.020	0.101	0.142	0.629	0.012	0.070	0.109	0.409	0.010	0.068	0.098	0.528
DT	0.031	0.101	0.176	0.430	0.014	0.057	0.117	0.324	0.007	0.043	0.085	0.643
LR	0.051	0.180	0.226	0.061	0.019	0.085	0.138	0.053	0.019	0.084	0.138	0.063
Ensemble Learning												
XGBoost	0.020	0.086	0.141	0.018	0.009	0.054	0.095	0.557	0.004	0.040	0.067	0.778
RF	0.022	0.090	0.147	-0.067	0.008	0.048	0.090	0.600	0.004	0.035	0.061	0.813
GB	0.018	0.083	0.135	0.101	0.010	0.054	0.099	0.513	0.009	0.054	0.095	0.558
AdaBoost	0.028	0.122	0.167	-0.386	0.012	0.068	0.108	0.419	0.013	0.081	0.116	0.333
Deep Learning												
LSTM	0.018	0.086	0.136	0.087	0.011	0.063	0.107	0.438	0.014	0.072	0.119	0.304
GRU	0.018	0.086	0.135	0.093	0.011	0.060	0.103	0.478	0.014	0.071	0.118	0.309
BWS												
Algorithm	**MSE**	**MAE**	**RMSE**	**R^2**	**MSE**	**MAE**	**RMSE**	**R^2**	**MSE**	**MAE**	**RMSE**	**R^2**
Machine Learning												
KNN	0.007	0.044	0.086	0.633	0.007	0.043	0.084	0.648	0.005	0.038	0.072	0.747
SVR	0.010	0.078	0.100	0.506	0.009	0.069	0.093	0.575	0.006	0.054	0.074	0.726
DT	0.012	0.053	0.111	0.386	0.012	0.051	0.108	0.425	0.005	0.037	0.073	0.733
LR	0.012	0.070	0.109	0.410	0.012	0.069	0.108	0.426	0.011	0.067	0.105	0.453
Ensemble Learning												
XGBoost	0.008	0.044	0.088	0.616	0.006	0.041	0.078	0.698	0.003	0.030	0.052	0.865
RF	0.007	0.044	0.085	0.646	0.006	0.041	0.076	0.716	0.003	0.030	0.052	0.867
GB	0.007	0.043	0.081	0.673	0.006	0.042	0.078	0.696	0.004	0.035	0.061	0.818
AdaBoost	0.008	0.055	0.090	0.598	0.008	0.055	0.090	0.600	0.007	0.058	0.085	0.641
Deep Learning												
LSTM	0.007	0.046	0.084	0.650	0.007	0.044	0.081	0.673	0.006	0.045	0.079	0.690
GRU	0.007	0.048	0.084	0.648	0.007	0.047	0.081	0.673	0.006	0.044	0.078	0.699

Table 15. Evaluation of Models on 1420 and 1424 Weather Station dataset in FC Prediction

1420												
	3-Features				5-Features				All-Features			
Algorithm	**MSE**	**MAE**	**RMSE**	**R^2**	**MSE**	**MAE**	**RMSE**	**R^2**	**MSE**	**MAE**	**RMSE**	**R^2**
ML												
KNN	0.003	0.034	0.055	0.389	0.002	0.028	0.047	0.550	0.002	0.023	0.041	0.667
SVR	0.006	0.069	0.079	-0.261	0.006	0.065	0.075	-0.134	0.004	0.053	0.062	0.219
DT	0.003	0.033	0.052	0.457	0.004	0.032	0.062	0.225	0.002	0.018	0.041	0.668
LR	0.005	0.060	0.069	0.046	0.005	0.059	0.069	0.058	0.005	0.059	0.068	0.066
Ensemble Learning												
XGBoost	0.003	0.033	0.052	0.457	0.002	0.027	0.046	0.567	0.001	0.016	0.028	0.839
RF	0.003	0.033	0.052	0.457	0.002	0.031	0.048	0.531	0.001	0.022	0.034	0.764
GB	0.003	0.034	0.052	0.455	0.003	0.034	0.051	0.474	0.002	0.032	0.048	0.539
AdaBoost	0.003	0.042	0.058	0.330	0.004	0.050	0.064	0.178	0.005	0.061	0.072	-0.049
DL												
LSTM	0.003	0.038	0.053	0.428	0.003	0.037	0.053	0.444	0.004	0.053	0.065	0.158
GRU	0.003	0.038	0.054	0.421	0.003	0.036	0.053	0.442	0.005	0.062	0.070	0.010
1424												
Algorithm	**MSE**	**MAE**	**RMSE**	**R^2**	**MSE**	**MAE**	**RMSE**	**R^2**	**MSE**	**MAE**	**RMSE**	**R^2**
ML												
KNN	0.003	0.033	0.052	0.457	0.002	0.024	0.043	0.632	0.001	0.020	0.037	0.732
SVR	0.003	0.034	0.055	0.389	0.003	0.027	0.056	0.372	0.002	0.017	0.039	0.689
DT	0.005	0.060	0.069	0.046	0.005	0.059	0.069	0.053	0.004	0.054	0.063	0.202
LR	0.006	0.069	0.079	-0.261	0.005	0.061	0.070	0.013	0.005	0.059	0.069	0.053
Ensemble Learning												
XGBoost	0.003	0.033	0.052	0.458	0.002	0.023	0.041	0.658	0.001	0.015	0.028	0.843
RF	0.003	0.033	0.052	0.457	0.002	0.028	0.044	0.607	0.001	0.022	0.035	0.757
GB	0.003	0.034	0.052	0.455	0.002	0.032	0.049	0.514	0.002	0.032	0.048	0.539
AdaBoost	0.003	0.042	0.059	0.307	0.004	0.053	0.065	0.161	0.006	0.065	0.078	-0.235
DL												
LSTM	0.003	0.038	0.054	0.424	0.003	0.042	0.055	0.391	0.004	0.051	0.063	0.198
GRU	0.003	0.036	0.054	0.414	0.003	0.036	0.052	0.466	0.003	0.037	0.054	0.420

Table 16. Evaluation of Models on 7341 and BWS Weather Station dataset in FC Prediction

7341												
	3-Features				5-Features				All-Features			
Algorithm	**MSE**	**MAE**	**RMSE**	**R^2**	**MSE**	**MAE**	**RMSE**	**R^2**	**MSE**	**MAE**	**RMSE**	**R^2**
ML												
KNN	0.003	0.034	0.055	0.389	0.003	0.031	0.051	0.486	0.002	0.026	0.043	0.626
SVR	0.006	0.069	0.079	-0.261	0.006	0.064	0.074	-0.108	0.004	0.054	0.063	0.200
DT	0.003	0.033	0.052	0.457	0.004	0.034	0.065	0.162	0.002	0.019	0.042	0.651
LR	0.005	0.060	0.069	0.046	0.005	0.059	0.069	0.057	0.005	0.059	0.069	0.057
Ensemble Learning												
XGBoost	0.003	0.033	0.052	0.457	0.002	0.029	0.047	0.551	0.001	0.016	0.029	0.826
RF	0.003	0.033	0.052	0.457	0.002	0.033	0.050	0.507	0.001	0.023	0.036	0.747
GB	0.003	0.034	0.052	0.455	0.003	0.034	0.052	0.468	0.002	0.032	0.048	0.536
AdaBoost	0.003	0.042	0.059	0.312	0.005	0.059	0.071	-0.002	0.005	0.062	0.073	-0.077
DL												
LSTM	0.003	0.038	0.053	0.428	0.003	0.039	0.054	0.415	0.004	0.056	0.066	0.124
GRU	0.003	0.037	0.053	0.430	0.003	0.037	0.053	0.434	0.005	0.063	0.071	-0.016

	BWS											
Algorithm	**MSE**	**MAE**	**RMSE**	**R^2**	**MSE**	**MAE**	**RMSE**	**R^2**	**MSE**	**MAE**	**RMSE**	**R^2**
ML												
KNN	0.002	0.026	0.046	0.582	0.001	0.020	0.036	0.737	0.001	0.018	0.034	0.773
SVR	0.003	0.040	0.054	0.408	0.002	0.023	0.047	0.564	0.001	0.018	0.039	0.703
DT	0.004	0.032	0.061	0.262	0.003	0.040	0.051	0.485	0.003	0.042	0.052	0.466
LR	0.004	0.057	0.067	0.109	0.003	0.039	0.053	0.434	0.003	0.039	0.052	0.453
Ensemble Learning												
XGBoost	0.002	0.026	0.044	0.610	0.001	0.018	0.033	0.778	0.001	0.014	0.027	0.856
RF	0.002	0.026	0.045	0.593	0.001	0.019	0.034	0.770	0.001	0.015	0.027	0.851
GB	0.002	0.026	0.046	0.568	0.001	0.022	0.038	0.718	0.001	0.020	0.035	0.756
AdaBoost	0.002	0.029	0.048	0.538	0.003	0.043	0.054	0.408	0.004	0.051	0.061	0.244
DL												
LSTM	0.002	0.029	0.046	0.580	0.002	0.026	0.040	0.678	0.002	0.029	0.044	0.618
GRU	0.002	0.028	0.045	0.588	0.002	0.026	0.040	0.686	0.002	0.024	0.039	0.695

5-5- Comparison with Existing Techniques

We emphasize comparing machine learning techniques specifically for predicting TC consumption (Table 17), as other aspects like cooling ventilation or free cooling present limited scope for comparison in existing studies due to factors such as different evaluation metrics, low-scale datasets, and insufficient granularity in temporal data analysis. This lack of scope highlights one of the novel contributions of our research. Table 17 summarizes the performance metrics of various models used for predicting TC consumption. Fan & Ding [49] provide RMSE values of 405.7 kW and an R^2 of 0.958 for their MNR model, though MSE and MAE metrics are not available, limiting a full assessment of their model's accuracy. He et al. [50] utilize an LSTM-ANN model, reporting an MAE of 111.95 and RMSE of 140.95 but omit MSE and R^2 values, which hampers a complete evaluation of their model's performance. Bekdaş et al. [51] present a GBR model with negative MSE (-8.9397), MAE (-1.7699), and RMSE (-2.9843) but achieves an R^2 of 0.9949 reflecting a high level of fit. Fan et al. [23] report an XGB model with an RMSE of 106.5 and an R^2 value but lacks MSE and MAE metrics, providing an incomplete view of its performance [23]. Myat et al. [52] use a MvFIF-PCA-LSTM model, showing an MAE of 9.06, RMSE of 0.015, and a very high R^2 of 99.68, with MSE not provided, suggesting exceptionally low error metrics. Our study, employing XGBoost, achieves an MSE of 0.011, MAE of 0.060, RMSE of 0.104, and an R^2 of 0.911, indicating strong performance with comprehensive metrics. This focus on TC consumption, as opposed to other aspects, underscores the novelty and detailed contribution of our research to the field.

Table 17. Comparing machine learning techniques

Reference	Year	Technique	MSE	MAE	RMSE	R^2
Fan & Ding [49]	2019	MNR	-	-	405.7 (kW)	0.95
He et al. [50]	2022	LSTM-ANN	-	111.95	140.95	-
Bekdaş et al. [51]	2023	GBR	-8.9397	-1.7699	-2.9843	0.99
Fan et al. [23]	2017	XGB		71.6	106.5	-
Myat et al. [52]	2024	MyFIF-PCA-LSTM	-	9.06	0.015	0.99
This study	2024	XGBoost	0.011	0.060	0.104	0.911

5-6- Discussion

This section discusses the performance of various models for predicting different cooling needs across weather stations. Starting from Cooling Consumption (CC), RF consistently emerged as the top performer for both stations 1420 and 1424 across all feature sets. This can be attributed to RF's ability to handle non-linear relationships and high-dimensional data effectively, leading to superior accuracy. Notably, in station 1424, RF achieved an R^2 value of 0.841 with all features, highlighting its strength in capturing complex data patterns. Regarding feature sets, including more features generally improved model performance, suggesting that a comprehensive set of variables enhances prediction by capturing nuanced data relationships. Station 1424 exhibited better results compared to station 1420, possibly due to differences in data quality or environmental factors influencing CC demands.

Moving to FC, XGBoost consistently demonstrated the best performance across all feature sets and weather stations for FC prediction. Its ensemble learning approach, combining the strengths of multiple DT, enables the effective capture of intricate data patterns, resulting in superior accuracy. In station 1424, XGBoost achieved an impressive R^2 value of 0.922 with all features, indicating its efficacy in predicting FC loads. A moderate number of features yielded optimal results for FC prediction, suggesting a balance between capturing relevant information and avoiding overfitting. Station 1424 again exhibited better performance than station 1420, suggesting potential variations in environmental conditions influencing FC requirements.

With respect to CV, several models, including SVR, RF, LSTM, and GRU, emerged as top performers for predicting CV across various datasets. SVR's strength lies in handling complex relationships and high-dimensional data, while RF's ensemble nature reduces overfitting. LSTM and GRU, as deep learning models, excel in capturing temporal dependencies, which is crucial for modeling CV dynamics. Key variables like temperature, humidity, airflow rate, and equipment status significantly impact prediction accuracy. The inclusion of comprehensive feature sets further enhances predictive power by offering a holistic view of system dynamics.

Finally, considering TC, similar to FC prediction, XGBoost emerged as the top performer across both weather stations, 7341 and BWS, achieving consistently high R^2 values across different feature sets. XGBoost's ensemble learning methodology allows it to handle complex data relationships, making it well-suited for TC prediction tasks. For instance, in station 7341, XGBoost achieved an R^2 value of 0.911 with all features, displaying its ability to accurately predict TC demands. Notably, a balanced selection of features, including both environmental and operational variables, contributed to the models' predictive efficacy. Station 7341 presented slightly better results compared to station BWS, indicating potential differences in cooling load dynamics influenced by location-specific factors.

More importantly, the scalability of these findings to other buildings or geographic locations with different climate conditions and building characteristics depends on several factors. While the models demonstrated strong performance for the ECB building, their effectiveness in other settings may vary due to differences in local weather patterns, building designs, and operational conditions. To enhance scalability, it would be beneficial to validate the models on diverse datasets from various geographic regions and building types.

The study acknowledges the complexity of machine learning models, particularly ensemble and deep learning approaches, which can pose challenges in terms of interpretability and practical application [53]. To ensure that the model's predictions are both understandable and actionable for building managers, the study emphasizes the use of feature importance metrics and sensitivity analysis to highlight the most influential factors driving the predictions, making it easier for managers to grasp key contributors to cooling demand.

6- Conclusion

This study has significantly advanced the field of cooling consumption forecasting by rigorously evaluating various ML and DL models to optimize energy management in interconnected HVAC systems. The analysis underscored the critical role of accurate predictions in enhancing the efficiency and sustainability of building energy systems. Our comprehensive evaluation utilized a diverse set of ML algorithms, including KNN, DT, SVR, LR, RF, GB, XGBoost, Adaboost, LSTM, and GRU models across multiple weather stations and feature sets. The study specifically focused on four key cooling systems: CC, CV, FC, and TC, leveraging data from four weather stations relevant to the ECB building in Frankfurt. The fundamental findings are as follows: Random Forest emerged as the strongest performer for overall cooling prediction, demonstrating its ability to capture intricate data relationships. XGBoost excelled in free cooling prediction, showcasing the efficacy of ensemble learning methods in this domain. Comprehensive feature sets significantly improved model performance by capturing the complex interactions between environmental and operational variables. Variations in performance across stations emphasized the influence of location-specific factors on cooling demand dynamics, highlighting the need for tailored prediction approaches.

Future research will consider advanced feature engineering techniques such as feature selection algorithms, dimensionality reduction, and domain-specific feature creation. This would allow models to identify the most influential variables, leading to improved accuracy and interpretability. Moreover, integrating real-time data from Internet of Things (IoT) sensors, weather forecasts, and building management systems would enable models to adapt dynamically to changing conditions. This would enhance predictive capabilities for optimized cooling load management.

7- Declarations

7-1- Author Contributions

Conceptualization, F.A., M.C., and N.C.R.; methodology, F.A.; software, F.A.; validation, M.C. and N.C.R.; formal analysis, F.A.; investigation, F.A.; resources, F.A.; data curation, F.A.; writing—original draft preparation, F.A.; writing—review and editing, M.C. and N.C.R.; visualization, F.A.; supervision, M.C. and N.C.R.; project administration, F.A., M.C., And N.C.R.; funding acquisition, M.C. and N.C.R. All authors have read and agreed to the published version of the manuscript.

7-2- Data Availability Statement

The data presented in this study are available on request from the corresponding author.

7-3- Funding

This work was supported by national funds through FCT (Fundação para a Ciência e a Tecnologia), under the project-UIDB/04152/2020 (doi:10.54499/UIDB/04152/2020)-Centro de Investigação em Gestão de Informação (MagIC)/NOVA IMS.

7-4- Institutional Review Board Statement

Not applicable.

7-5- Informed Consent Statement

Not applicable.

7-6- Conflicts of Interest

The authors declare that there is no conflict of interest regarding the publication of this manuscript. In addition, the ethical issues, including plagiarism, informed consent, misconduct, data fabrication and/or falsification, double publication and/or submission, and redundancies have been completely observed by the authors.

8- References

[1] Almuhaini, S. H., & Sultana, N. (2023). Forecasting Long-Term Electricity Consumption in Saudi Arabia Based on Statistical and Machine Learning Algorithms to Enhance Electric Power Supply Management. Energies, 16(4), 2035. doi:10.3390/en16042035.

[2] Zou, X., Wang, R., Hu, G., Rong, Z., & Li, J. (2022). CO_2 Emissions Forecast and Emissions Peak Analysis in Shanxi Province, China: An Application of the LEAP Model. Sustainability (Switzerland), 14(2), 637. doi:10.3390/su14020637.

[3] Jena, P. R., Managi, S., & Majhi, B. (2021). Forecasting the CO_2 emissions at the global level: A multilayer artificial neural network modelling. Energies, 14(19), 1–23. doi:10.3390/en14196336.

[4] IEA. (2024). Energy system Buildings: IEA 50. International Energy Agency (IEA), Paris, France. Available online: https://www.iea.org/energy-system/buildings (accessed on November 2024).

[5] European Parliament. (2023). P9_TA(2023)0068 Energy performance of buildings (recast). European Parliament, Strasbourg, France, Vol. 0426, No. March 2023.

[6] Piazolo, D. (2022). The Paris Climate Agreement as Benchmark for Buildings and Companies. IOP Conference Series: Earth and Environmental Science, 1078(1), 012115. doi:10.1088/1755-1315/1078/1/012115.

[7] Muhamad, W. N. W., Zain, M. Y. M., Wahab, N., Aziz, N. H. A., & Kadir, R. A. (2010). Energy efficient lighting system design for building. ISMS 2010 - UKSim/AMSS 1st International Conference on Intelligent Systems, Modelling and Simulation, 282–286. doi:10.1109/ISMS.2010.59.

[8] Yang, Y., Hu, G., & Spanos, C. J. (2022). Stochastic Optimal Control of HVAC System for Energy-Efficient Buildings. IEEE Transactions on Control Systems Technology, 30(1), 376–383. doi:10.1109/TCST.2021.3057630.

[9] Rocha, P., Siddiqui, A., & Stadler, M. (2015). Improving energy efficiency via smart building energy management systems: A comparison with policy measures. Energy and Buildings, 88, 203–213. doi:10.1016/j.enbuild.2014.11.077.

[10] Sekaranom, A. B., Nurjani, E., Harini, R., & Muttaqin, A. S. (2020). Simulation of daily rainfall data using articulated weather generator model for seasonal prediction of ENSO-affected zones in Indonesia. Indonesian Journal of Geography, 35(2), 143–153. doi:10.22146/ijg.50862.

[11] Moradzadeh, A., Mansour-Saatloo, A., Mohammadi-Ivatloo, B., & Anvari-Moghaddam, A. (2020). Performance evaluation of two machine learning techniques in heating and cooling loads forecasting of residential buildings. Applied Sciences (Switzerland), 10(11), 3829. doi:10.3390/app10113829.

[12] Kathiriya Siddhartha Nuthakki, S. (2023). AI and the Future of Medicine: Pioneering Drug Discovery with Language Models. International Journal of Science and Research (IJSR), 12(3), 1824-1829. doi:10.21275/sr24304173757.

[13] Kim, D., Lee, Y., Chin, K., Mago, P. J., Cho, H., & Zhang, J. (2023). Implementation of a Long Short-Term Memory Transfer Learning (LSTM-TL)-Based Data-Driven Model for Building Energy Demand Forecasting. Sustainability (Switzerland), 15(3), 2340. doi:10.3390/su15032340.

[14] Zeferina, V., Birch, C., Edwards, R., & Wood, R. (2019). Sensitivity analysis of peak and annual space cooling load at simplified office dynamic building model. E3S Web of Conferences, 111(201 9), 4–11. doi:10.1051/e3sconf/201911104038.

[15] Shin, M., & Do, S. L. (2016). Prediction of cooling energy use in buildings using an enthalpy-based cooling degree days method in a hot and humid climate. Energy and Buildings, 110, 57–70. doi:10.1016/j.enbuild.2015.10.035.

[16] Zhao, X., Yin, Y., Zhang, S., & Xu, G. (2023). Data-driven prediction of energy consumption of district cooling systems (DCS) based on the weather forecast data. Sustainable Cities and Society, 90, 104382. doi:10.1016/j.scs.2022.104382.

[17] Dong, F., Yu, J., Quan, W., Xiang, Y., Li, X., & Sun, F. (2022). Short-term building cooling load prediction model based on DwdAdam-ILSTM algorithm: A case study of a commercial building. Energy and Buildings, 272, 112337. doi:10.1016/j.enbuild.2022.112337.

[18] Nuthakki, S., Kumar, S., Kulkarni, C. S., & Nuthakki, Y. (2022). Role of AI Enabled Smart Meters to Enhance Customer Satisfaction. International Journal of Computer Science and Mobile Computing, 11(12), 99–107. doi:10.47760/ijcsmc.2022.v11i12.010.

[19] Nuthakki, S., Kulkarni, C. S., Kathiriya, S., & Nuthakki, Y. (2024). Artificial Intelligence Applications in Natural Gas Industry: A Literature Review. International Journal of Engineering and Advanced Technology, 13(3), 64–70. doi:10.35940/ijeat.c4383.13030224.

[20] Sadeghian Broujeny, R., Ben Ayed, S., & Matalah, M. (2023). Energy Consumption Forecasting in a University Office by Artificial Intelligence Techniques: An Analysis of the Exogenous Data Effect on the Modeling. Energies, 16(10), 4065. doi:10.3390/en16104065.

[21] Lu, S., Cui, M., Gao, B., Liu, J., Ni, J., Liu, J., & Zhou, S. (2024). A Comparative Analysis of Machine Learning Algorithms in Predicting the Performance of a Combined Radiant Floor and Fan Coil Cooling System. Buildings, 14(6), 1659. doi:10.3390/buildings14061659.

[22] Bedi, J., & Toshniwal, D. (2019). Deep learning framework to forecast electricity demand. Applied Energy, 238, 1312–1326. doi:10.1016/j.apenergy.2019.01.113.

[23] Fan, C., Xiao, F., & Zhao, Y. (2017). A short-term building cooling load prediction method using deep learning algorithms. Applied Energy, 195, 222–233. doi:10.1016/j.apenergy.2017.03.064.

[24] Li, A., Xiao, F., Zhang, C., & Fan, C. (2021). Attention-based interpretable neural network for building cooling load prediction. Applied Energy, 299. doi:10.1016/j.apenergy.2021.117238.

[25] Lopes, M. N., & Lamberts, R. (2018). Development of a metamodel to predict cooling energy consumption of HVAC systems in office buildings in different climates. Sustainability (Switzerland), 10(12), 4718. doi:10.3390/su10124718.

[26] Amasyali, K., & El-Gohary, N. (2021). Machine learning for occupant-behavior-sensitive cooling energy consumption prediction in office buildings. Renewable and Sustainable Energy Reviews, 142, 110714. doi:10.1016/j.rser.2021.110714.

[27] Mui, K. W., Satheesan, M. K., & Wong, L. T. (2022). Building cooling energy consumption prediction with a hybrid simulation Approach: Generalization beyond the training range. Energy and Buildings, 276, 112502. doi:10.1016/j.enbuild.2022.112502.

[28] Moon, J. W., Jung, S. K., Lee, Y. O., & Choi, S. (2015). Prediction performance of an artificial neural network model for the amount of cooling energy consumption in hotel rooms. Energies, 8(8), 8226–8243. doi:10.3390/en8088226.

[29] Borowski, M., & Zwolińska, K. (2020). Prediction of cooling energy consumption in hotel building using machine learning techniques. Energies, 13(23), 6226. doi:10.3390/en13236226.

[30] Lu, C., Li, S., Reddy Penaka, S., & Olofsson, T. (2023). Automated machine learning-based framework of heating and cooling load prediction for quick residential building design. Energy, 274(February), 127334. doi:10.1016/j.energy.2023.127334.

[31] Liu, C. L., Tseng, C. J., Huang, T. H., Yang, J. S., & Huang, K. Bin. (2023). A multi-task learning model for building electrical load prediction. Energy and Buildings, 278, 112601. doi:10.1016/j.enbuild.2022.112601.

[32] Zhang, C., Tian, X., Zhao, Y., & Lu, J. (2023). Automated machine learning-based building energy load prediction method. Journal of Building Engineering, 80(October), 108071. doi:10.1016/j.jobe.2023.108071.

[33] Pavlatos, C., Makris, E., Fotis, G., Vita, V., & Mladenov, V. (2023). Utilization of Artificial Neural Networks for Precise Electrical Load Prediction. Technologies, 11(3), 1–14. doi:10.3390/technologies11030070.

[34] Tsalikidis, N., Mystakidis, A., Tjortjis, C., Koukaras, P., & Ioannidis, D. (2024). Energy load forecasting: one-step ahead hybrid model utilizing ensembling. Computing, Springer, Vienna, Austria. doi:10.1007/s00607-023-01217-2.

[35] Guo, G., Wang, H., Bell, D., Bi, Y., & Greer, K. (2003). KNN model-based approach in classification. On the Move to Meaningful Internet Systems 2003: CoopIS, DOA, and ODBASE: OTM Confederated International Conferences, CoopIS, DOA, and ODBASE 2003, Catania, Sicily, Italy, November 3-7, 2003. doi:10.1007/978-3-540-39964-3_62.

[36] Zhang, F., & O'Donnell, L. J. (2020). Support vector regression. Machine Learning: Methods and Applications to Brain Disorders, 123-140. doi:10.1016/B978-0-12-815739-8.00007-9.

[37] Myles, A. J., Feudale, R. N., Liu, Y., Woody, N. A., & Brown, S. D. (2004). An introduction to decision tree modeling. Journal of Chemometrics, 18(6), 275–285. doi:10.1002/cem.873.

[38] Su, X., Yan, X., & Tsai, C. L. (2012). Linear regression. Wiley Interdisciplinary Reviews: Computational Statistics, 4(3), 275–294. doi:10.1002/wics.1198.

[39] Chen, T., & Guestrin, C. (2016). XGBoost: A scalable tree boosting system. Proceedings of the ACM SIGKDD International Conference on Knowledge Discovery and Data Mining, 13-17-August-2016, 785–794. doi:10.1145/2939672.2939785.

[40] Jin, Z., Shang, J., Zhu, Q., Ling, C., Xie, W., & Qiang, B. (2020). RFRSF: Employee Turnover Prediction Based on Random Forests and Survival Analysis. Lecture Notes in Computer Science (Including Subseries Lecture Notes in Artificial Intelligence and Lecture Notes in Bioinformatics), 12343 LNCS, 503–515. doi:10.1007/978-3-030-62008-0_35.

[41] Natekin, A., & Knoll, A. (2013). Gradient boosting machines, a tutorial. Frontiers in Neurorobotics, 7(Dec), 1-21. doi:10.3389/fnbot.2013.00021.

[42] Solomatine, D. P., & Shrestha, D. L. (2004). AdaBoost.RT: A boosting algorithm for regression problems. IEEE International Conference on Neural Networks - Conference Proceedings, 2, 1163–1168. doi:10.1109/ijcnn.2004.1380102.

[43] Gers, F. A., Schmidhuber, J., & Cummins, F. (2000). Learning to forget: Continual prediction with LSTM. Neural computation, 12(10), 2451-2471. doi:10.1162/089976600300015015.

[44] Yao, K., Cohn, T., Vylomova, K., Duh, K., & Dyer, C. (2015). Depth-gated Recurrent Neural Networks. arXiv preprint arXiv:1508.03790. doi:10.48550/arXiv.1508.03790.

[45] Alaraj, M., Kumar, A., Alsaidan, I., Rizwan, M., & Jamil, M. (2021). Energy Production Forecasting from Solar Photovoltaic Plants Based on Meteorological Parameters for Qassim Region, Saudi Arabia. IEEE Access, 9, 83241–83251. doi:10.1109/ACCESS.2021.3087345.

[46] Dadhich, M., Pahwa, M. S., Jain, V., & Doshi, R. (2021). Predictive Models for Stock Market Index Using Stochastic Time Series ARIMA Modeling in Emerging Economy. Lecture Notes in Mechanical Engineering, 281–290. doi:10.1007/978-981-16-0942-8_26.

[47] Shrivastava, S., Bal, P. K., Ashrit, R., Sharma, K., Lodh, A., & Mitra, A. K. (2017). Performance of NCUM global weather modeling system in predicting the extreme rainfall events over the central India during the Indian summer monsoon 2016. Modeling Earth Systems and Environment, 3(4), 1409–1419. doi:10.1007/s40808-017-0387-8.

[48] Brahimi, T. (2019). Using artificial intelligence to predict wind speed for energy application in Saudi Arabia. Energies, 12(24), 4669. doi:10.3390/en12244669.

[49] Fan, C., & Ding, Y. (2019). Cooling load prediction and optimal operation of HVAC systems using a multiple nonlinear regression model. Energy and Buildings, 197, 7–17. doi:10.1016/j.enbuild.2019.05.043.

[50] He, N., Liu, L., Chu, D., & Qian, C. (2022). Air Conditioning Cooling Load Prediction Based on LSTM-ANN. 2022 5th International Symposium on Autonomous Systems, ISAS 2022, 1–6. doi:10.1109/ISAS55863.2022.9757345.

[51] Bekdaş, G., Aydın, Y., Isıkdağ, Ü., Sadeghifam, A. N., Kim, S., & Geem, Z. W. (2023). Prediction of Cooling Load of Tropical Buildings with Machine Learning. Sustainability (Switzerland), 15(11), 9061. doi:10.3390/su15119061.

[52] Myat, A., Kondath, N., Soh, Y. L., & Hui, A. (2024). A hybrid model based on multivariate fast iterative filtering and long short-term memory for ultra-short-term cooling load prediction. Energy and Buildings, 307, 113977. doi:10.1016/j.enbuild.2024.113977.

[53] Jo, Y. Y., Cho, Y., Lee, S. Y., Kwon, J. Myoung, Kim, K. H., Jeon, K. H., Cho, S., Park, J., & Oh, B. H. (2021). Explainable artificial intelligence to detect atrial fibrillation using electrocardiogram. International Journal of Cardiology, 328, 104–110. doi:10.1016/j.ijcard.2020.11.053.